



Australian Government
Bureau of Meteorology

The Centre for Australian Weather and Climate Research
A partnership between CSIRO and the Bureau of Meteorology



Assessment of POAMA's predictions of some climate indices for use as predictors of Australian rainfall

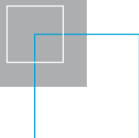
Sally Langford, Harry H. Hendon and Eun-Pa Lim

CAWCR Technical Report No. 031

April 2011



www.cawcr.gov.au



Assessment of POAMA's predictions of some climate indices for use as predictors of Australian rainfall

Sally Langford, Harry H. Hendon and Eun-Pa Lim

*The Centre for Australian Weather and Climate Research
- a partnership between CSIRO and the Bureau of Meteorology*

CAWCR Technical Report No. 031

April 2011

ISSN: 1836-019X

National Library of Australia Cataloguing-in-Publication entry

- Authors: Langford, S., Hendon, H.H. and Lim, E-P
- Title: Assessment of POAMA's predictions of some climate indices for use as predictors of Australian rainfall. [Electronic Resource]
- ISBN: 978-1-921826-07-8 (PDF)
- Series: CAWCR technical report, 31
- Notes: Includes bibliographical references and index.
- Subjects: Climate indices for Australian rainfall
- Other Authors/Contributors: Sally Langford, Harry H. Hendon and Eun-Pa Lim.
- Dewey Number: 551.5246

Enquiries should be addressed to:
Sally Langford
Centre for Australian Weather and Climate Research:
A partnership between the Bureau of Meteorology and CSIRO
GPO Box 1289, Melbourne
Victoria 3001, Australia

S.Langford@bom.gov.au

Copyright and Disclaimer

© 2011 CSIRO and the Bureau of Meteorology. To the extent permitted by law, all rights are reserved and no part of this publication covered by copyright may be reproduced or copied in any form or by any means except with the written permission of CSIRO and the Bureau of Meteorology.

CSIRO and the Bureau of Meteorology advise that the information contained in this publication comprises general statements based on scientific research. The reader is advised and needs to be aware that such information may be incomplete or unable to be used in any specific situation. No reliance or actions must therefore be made on that information without seeking prior expert professional, scientific and technical advice. To the extent permitted by law, CSIRO and the Bureau of Meteorology (including each of its employees and consultants) excludes all liability to any person for any consequences, including but not limited to all losses, damages, costs, expenses and any other compensation, arising directly or indirectly from using this publication (in part or in whole) and any information or material contained in it.

Water Information Research and Development Alliance (WIRADA)
Project 4.2 “Improved climate predictions at hydrologically-relevant time and space scales from the POAMA seasonal climate forecasts.”

This research was supported in part by the South Eastern Australian Climate Initiative (SEACI:<http://www.seaci.org>; Advancing Seasonal Predictions for SEA)

CONTENTS

1	Abstract	1
2	Introduction	1
3	Observational and forecast data	1
3.1	Observed data	2
3.2	POAMA forecast data	2
3.2.1	POAMA grid	2
3.2.2	Persistence	3
3.2.3	RMSE skill score	3
3.2.4	Climate indices	3
4	Predicting Indices with POAMA	6
4.1	Relationship with rainfall	10
4.2	Cross correlation of observed indices	13
5	Assessment of skill	14
5.1	Maximum skill plots	15
6	Conclusion	22
	References	23
	Appendix - A	25

LIST OF FIGURES

Fig. 1	Regression of observed index onto observed SST anomalies (panels (a) to (f)), observed MSLP anomalies (panels (g) and (h)), and observed 500hPa U wind anomalies (panel (i)) for SON. The black boxes in panel (a) show the locations of the Indian Ocean West and East Pole indices. The DMI is the difference between the SST anomalies in these regions. The white boxes in panels (b), (d) and (f) show the regions of the SST anomalies measured by the NINO indices. The black boxes in panel (c) show the three regions considered in the EMI index. The small black box to the north of Australia in panel (e) shows the location of the Indonesian Index region. The black boxes in panel (g) show the two regions over which the equatorial SOI is determined. SAM is the difference in the normalised monthly zonal MSLP at the latitudes indicated by the horizontal black lines in panel (h). The 140°E Blocking Index is the difference between the 500hPa zonal wind at the latitudes indicated by the black triangles in panel (i).	5
Fig. 2	Correlation of observed and predicted seasonal mean indices, for 1980-2006 and a lead time of 0 months. The season indicated on the x-axis is the verification season. ..	7
Fig. 3	Correlation of observed and predicted seasonal mean indices, for 1980-2006 and a lead time of 1 month. The season indicated on the x-axis is the verification season.	8
Fig. 4	Correlation of observed and predicted seasonal mean indices, for 1980-2006 and a lead time of 2 months. The season indicated on the x-axis is the verification season. ..	9
Fig. 5	Regression of observed index standardized anomalies onto observed rainfall anomalies for 1980-2006. Only regression coefficients with significance greater than 90 per cent are shown.....	11
Fig. 6	(a) Regression of DMI index with rainfall anomalies. (b) Partial regression of DMI index with rainfall anomalies, with NINO3 contribution to co-variability removed. (c) Partial regression of NINO3 index with rainfall anomalies, with DMI contribution to co-variability removed. (d) Regression of NINO3 index with rainfall anomalies. All regression coefficients for SON, 1980-2006.	12
Fig. 7	(a) Regression of NINO3 index with rainfall anomalies. (b) Partial regression of NINO3 index with rainfall anomalies, with NINO4 contribution to co-variability removed. (c) Partial regression of NINO4 index with rainfall anomalies, with NINO3 contribution to co-variability removed. (d) Regression of NINO4 index with rainfall anomalies. All regression coefficients for SON, 1980-2006.....	12
Fig. 8	RMSE skill score for predicting Australian rainfall with POAMA version p15b, compared to climatology for lead time 0 months. Results shown for DMI and NINO4 indices and the POAMA direct rainfall forecast. 1980-2006.	14
Fig. 9	Colours indicate the index with the highest RMSE skill score, for POAMA model version p15b compared to climatology, at lead time 0 months. 'Clim' refers to no index having a smaller RMSE than forecast by climatology. 'Pers' refers to persistence having the highest RMSE skill score. 'Poama' refers to the POAMA rainfall anomaly forecast having the highest RMSE skill score.....	17
Fig. 10	Colours indicate the index with the highest RMSE skill score, for POAMA model version p24 compared to climatology, at lead time 0 months. 'Clim' refers to no index having a smaller RMSE than forecast by climatology. 'Pers' refers to persistence having the highest RMSE skill score. 'Poama' refers to the POAMA rainfall anomaly forecast having the highest RMSE skill score.	18
Fig. 11	The RMSE skill score corresponding to Fig. 9 - the highest RMSE skill score for all indices, climatology, persistence and POAMA forecasts. For POAMA model version p15b compared to climatology, at lead time 0 months.....	19

Fig. 12	The RMSE skill score corresponding to Fig. 10 - the highest RMSE skill score for all indices, climatology, persistence and POAMA forecasts. For POAMA model p24 compared to climatology, at lead time 0 months.	20
Fig. 13	Prediction of Australian rainfall with highest RMSE skill score, compared to climatology, as in Fig. 10, but for a select number of indices. Results for POAMA model version p15b, 1980-2006, lead time 0 months.	21

LIST OF FIGURES IN APPENDIX - A

Fig. A.1	Autumn, regression of standardized anomalies of the observed indices onto observed rainfall anomalies for 1980-2006. Only regression coefficients with significance greater than 90 per cent are shown.	25
Fig. A.2	Winter, regression of standardized anomalies of the observed indices onto observed rainfall anomalies for 1980-2006. Only regression coefficients with significance greater than 90 per cent are shown.	26
Fig. A.3	Spring, regression of standardized anomalies of the observed indices onto observed rainfall anomalies for 1980-2006. Only regression coefficients with significance greater than 90 per cent are shown.	27
Fig. A.4	Summer, regression of standardized anomalies of the observed indices onto observed rainfall anomalies for 1980-2006. Only regression coefficients with significance greater than 90 per cent are shown.	28
Fig. A.5	RMSE skill score for predicting Australian rainfall with POAMA predicted indices, compared to climatological rainfall, for JFM. Results for p15b, 1980-2006.	29
Fig. A.6	RMSE skill score for predicting Australian rainfall with POAMA predicted indices, compared to climatological rainfall, for FMA. Results for p15b, 1980-2006.	30
Fig. A.7	RMSE skill score for predicting Australian rainfall with POAMA predicted indices, compared to climatological rainfall, for MAM. Results for p15b, 1980-2006.	31
Fig. A.8	RMSE skill score for predicting Australian rainfall with POAMA predicted indices, compared to climatological rainfall, for AMJ. Results for p15b, 1980-2006.	32
Fig. A.9	RMSE skill score for predicting Australian rainfall with POAMA predicted indices, compared to climatological rainfall, for MJJ. Results for p15b, 1980-2006.	33
Fig. A.10	RMSE skill score for predicting Australian rainfall with POAMA predicted indices, compared to climatological rainfall, for JJA. Results for p15b, 1980-2006.	34
Fig. A.11	RMSE skill score for predicting Australian rainfall with POAMA predicted indices, compared to climatological rainfall, for JAS. Results for p15b, 1980-2006.	35
Fig. A.12	RMSE skill score for predicting Australian rainfall with POAMA predicted indices, compared to climatological rainfall, for ASO. Results for p15b, 1980-2006.	36
Fig. A.13	RMSE skill score for predicting Australian rainfall with POAMA predicted indices, compared to climatological rainfall, for SON. Results for p15b, 1980-2006.	37
Fig. A.14	RMSE skill score for predicting Australian rainfall with POAMA predicted indices, compared to climatological rainfall, for OND. Results for p15b, 1980-2006.	38
Fig. A.15	RMSE skill score for predicting Australian rainfall with POAMA predicted indices, compared to climatological rainfall, for NDJ. Results for p15b, 1980-2006.	39
Fig. A.16	RMSE skill score for predicting Australian rainfall with POAMA predicted indices, compared to climatological rainfall, for DJF. Results for p15b, 1980-2006.	40
Fig. A.17	RMSE skill score for predicting Australian rainfall with POAMA predicted indices, compared to climatological rainfall, for JFM. Results for p24, 1980-2006.	41

Fig. A.18	RMSE skill score for predicting Australian rainfall with POAMA predicted indices, compared to climatological rainfall, for FMA. Results for p24, 1980-2006.	42
Fig. A.19	RMSE skill score for predicting Australian rainfall with POAMA predicted indices, compared to climatological rainfall, for MAM. Results for p24, 1980-2006.	43
Fig. A.20	RMSE skill score for predicting Australian rainfall with POAMA predicted indices, compared to climatological rainfall, for AMJ. Results for p24, 1980-2006.	44
Fig. A.21	RMSE skill score for predicting Australian rainfall with POAMA predicted indices, compared to climatological rainfall, for MJJ. Results for p24, 1980-2006.	45
Fig. A.22	RMSE skill score for predicting Australian rainfall with POAMA predicted indices, compared to climatological rainfall, for JJA. Results for p24, 1980-2006.	46
Fig. A.23	RMSE skill score for predicting Australian rainfall with POAMA predicted indices, compared to climatological rainfall, for JAS. Results for p24, 1980-2006.	47
Fig. A.24	RMSE skill score for predicting Australian rainfall with POAMA predicted indices, compared to climatological rainfall, for ASO. Results for p24, 1980-2006.	48
Fig. A.25	RMSE skill score for predicting Australian rainfall with POAMA predicted indices, compared to climatological rainfall, for SON. Results for p24, 1980-2006.	49
Fig. A.26	RMSE skill score for predicting Australian rainfall with POAMA predicted indices, compared to climatological rainfall, for OND. Results for p24, 1980-2006.	50
Fig. A.27	RMSE skill score for predicting Australian rainfall with POAMA predicted indices, compared to climatological rainfall, for NDJ. Results for p24, 1980-2006.	51
Fig. A.28	RMSE skill score for predicting Australian rainfall with POAMA predicted indices, compared to climatological rainfall, for DJF. Results for p24, 1980-2006.	52
Fig. A.29	Prediction of Australian rainfall with highest RMSE skill score, compared to climatology. The corresponding highest RMSE skill score for each grid point is shown on the right. Results for POAMA version p15b, 1980-2006. Significance limit of 90 per cent.	53
Fig. A.30	Prediction of Australian rainfall with highest RMSE skill score, compared to climatology. The corresponding highest RMSE skill score for each grid point is shown on the right. Results for POAMA version p24, 1980-2006. Significance limit of 90 per cent.	54

LIST OF TABLES IN APPENDIX A

Table 1. Cross correlation of observed indices for JFM.	55
Table 2. Cross correlation of observed indices for FMA.	55
Table 3. Cross correlation of observed indices for MAM.	56
Table 4. Cross correlation of observed indices for AMJ.	56
Table 5. Cross correlation of observed indices for MJJ.	57
Table 6. Cross correlation of observed indices for JJA.	57
Table 7. Cross correlation of observed indices for JAS.	58
Table 8. Cross correlation of observed indices for ASO.	58
Table 9. Cross correlation of observed indices for SON.	59
Table 10. Cross correlation of observed indices for OND.	59
Table 11. Cross correlation of observed indices for NDJ.	60
Table 12. Cross correlation of observed indices for DJF.	60

1 ABSTRACT

The Predictive Ocean Atmosphere Model for Australia (POAMA) coupled model forecast system has demonstrable skill for predicting rainfall at lead times of up to about 1 season (e.g. Lim et al. 2009). However, the predicted rainfall from POAMA may not be of sufficient accuracy and reliability to be useful for applications to hydrological prediction. This report explores using standard sea surface temperature, sea level pressure and tropospheric wind indices, which are highly correlated with rainfall and for which POAMA has good forecast skill, as potential input predictors in statistical rainfall forecast systems. The skill of each index for predicting Australian seasonal rainfall anomalies is assessed and those indices that provide the highest skill are flagged, as are the regions where the direct predictions of rainfall from POAMA are superior. For lead times of up to 2 months, we show additional benefit could be achieved from using a standard El Niño/Southern Oscillation (ENSO) index (e.g. NINO3), the Modoki El Niño Index (EMI), the Dipole Mode Index (DMI), and 140°E Blocking and Southern Annular Mode (SAM) indices.

2 INTRODUCTION

The direct output from the POAMA1.5/2 coupled model forecast system has demonstrable skill for predicting rainfall especially in eastern and southern Australia at lead times of up to about 1 season (e.g. Lim et al. 2009). Although the skill of these forecasts may be better than those produced by the operational statistical scheme run routinely at the National Climate Centre, the predicted rainfall from POAMA may not be of sufficient accuracy and reliability to be useful for application to hydrological prediction. An alternative approach may be to use predictions from POAMA of other climate indices that are highly correlated with rainfall and for which POAMA does have good forecast skill (e.g. the NINO3 index). These predicted indices then might possibly be of utility in empirical prediction schemes of relevance to hydrological applications. This report explores using POAMA forecasts of some standard climate indices of sea surface temperature, sea level pressure and tropospheric winds that have an established relationship with rainfall across Australia and thus could be used as potential input predictors in statistical rainfall forecast systems.

Details are given of the construction of the selected indices of sea surface temperature (SST), sea level pressure and tropospheric wind indices based on observational and model forecasts. The historical relationship of observed rainfall with the selected predictors is explored. The skill of each index for predicting Australian seasonal rainfall anomalies is assessed and those indices that provide the highest skill are flagged, as are the regions where the direct predictions of rainfall from POAMA are superior.

3 OBSERVATIONAL AND FORECAST DATA

The work reported here is based on forecasts and verification for the period 1980-2006. We exclusively will analyse seasonal mean forecasts and observations in this work. Seasonal mean refers here to the average of consecutive three months using monthly mean data. The summer seasons NDJ and DJF are based on averages of the monthly means from November and December of year 0 (1980-2006) and January and February of year 1 (1981-2007). For the forecasts from POAMA, lead time is defined as the number of months between the initialization

month and the first verification month. In other words, a prediction for SON at a lead time of 0 months uses the prediction initialized at the start of September. A lead time of 1 month uses the prediction initialized at the start of August.

3.1 Observed data

Observed rainfall for Australia for 1980-2006 is taken from the National Climate Centre's (NCC) gridded monthly analysis (Jones and Weymouth 1997). These analyses are on a 0.25x0.25 degree longitude-latitude grid in the range 44.5°S-10°S, 112°E-156.25°E.

Observed monthly mean sea level pressure and U wind at 500 hPa is taken from the NCEP reanalysis for 1980-2006 (Kalnay et al. 1996). The data is unpacked before calculating seasonal means. These global data are on a 2.5x2.5 degree longitude-latitude grid.

Observed monthly mean sea surface temperature is taken from the Hadley Centre Sea Ice and Sea Surface Temperature data set (HadISST; Rayner et al. 2003). These analyses are provided on 1.0x1.0 degree longitude-latitude grid.

3.2 POAMA forecast data

The p24 version of POAMA combines 10 member ensembles from each of the POAMA model versions p24a, p24b and p24c. The model version climatology (which is a function of start month and lead time) is subtracted from the individual members of each version of the model, before combining into a 30 member ensemble. The variance is not adjusted. The p15b version of the model is a 10 member ensemble (e.g. Zhao and Hendon 2009; Hudson et al. 2011). The main difference between p15b and p24 is the new ocean data assimilation in p24 (Yin et al. 2010). Forecast performance is similar for p24 and p15b, with p24 showing improved prediction for El Niño at longer lead times. Performance over continental Australia is similar in both versions. All results are based on hindcasts that are initialized on the first of each month for 1980-2006. Unless otherwise noted, we will assess forecast skill using the ensemble mean forecast. As this is an exploratory project, we will concentrate on relatively short lead time forecasts (0-2 month lead). Exploration of longer lead forecasts can be assessed if the present results are deemed useful.

When assessing the forecast skill, all statistical relationships are cross validated. This includes computation of the model climatology, means and medians. Cross validation is performed by leaving out the verifying year in order to compute statistical relationships based on the remaining 26 years.

3.2.1 POAMA grid

The POAMA output grid is coarser than the NCC grid used for verification of rainfall. Therefore, to compare the RMSE skill score at each of the finer grid points, the rainfall forecast on the native grid of POAMA is subdivided into the finer NCC grid. In other words, the 2.5x2.5 degree cell from POAMA (where the grid reference is in the centre of the cell in the longitude and latitude direction) is subdivided into 100 equal 0.25x0.25 degree cells (where the grid reference is in the centre of the cell in the longitude and latitude direction), each with the same forecast rainfall anomaly.

3.2.2 Persistence

Forecast skill from the dynamical model is also compared to a forecast generated by persisting the initial anomaly. For a 0 month lead time forecast, persistence in Australian rainfall is calculated using the monthly mean observed rainfall anomaly for the month immediately preceding the start of the target season. The monthly mean for the month before that is used for a lead time of 1 month. E.g. persistence of rainfall anomalies in the season SON uses the monthly mean observed rainfall from August for a lead time of 0 months, July for a lead time of 1 month, June for a lead time of 2 months.

3.2.3 RMSE skill score

Forecast skill is assessed with the Root Mean Square Error (RMSE) Skill Score, which is a measure of the improvement of a forecast above the reference forecast in terms of RMSE. The RMSE measures the average magnitude of the forecast error. The RMSE is calculated from the square root of the mean over all years of the squared difference between the predicted (ensemble mean) and observed rainfall anomaly:

$$\text{RMSE} = \sqrt{\frac{1}{N} \sum_{i=1}^N (X_i - Y_i)^2}, \quad (1)$$

where N is the number of years, X_i is the predicted ensemble mean rainfall anomaly, Y_i is the observed rainfall anomaly. In order to compare the forecast to a climatological forecast, the RMSE skill score is calculated. The RMSE skill score is 1 minus the ratio of the RMSE of the forecast compared to the RMSE of the reference forecast.

$$\text{RMSE Skill Score} = 1 - (\text{RMSE}/\text{RMSE}_{\text{ref}}), \quad (2)$$

where the RMSE_{ref} term is calculated via Eqn 1, where X_i is now the climatological rainfall anomaly, equal to zero. Although RMSE might not be an ideal skill score in all cases, the results here based on RMSE should be indicative of results based on other skill measures. For example, areas of high RMSE skill correspond to significant correlations between the predicted ensemble rainfall anomaly and the observed rainfall anomaly.

3.2.4 Climate indices

We use a number of standard indices that have a well established relationship with Australian rainfall. An advantage of using existing climate indices as possible predictors of rainfall is that the physical relationship with rainfall has been established. A disadvantage is that many of the standard indices exhibit covariance amongst themselves. The non-independence of the indices means that predictive skill of using multiple indices will be lower than the sum of the skills individually. Furthermore, care needs to be taken to avoid artificial skill if combinations of co-varying predictors are used. We demonstrate some of the subtleties of the inter-dependence of the indices in the following section.

Many of the standard climate indices focus on ENSO. The Southern Oscillation Index (SOI) is a measure of the standardized anomaly of difference in the mean sea level pressure (MSLP) between Tahiti (17.5°S, 210°E) and Darwin (12.5°S, 130°E; Troup 1965). The SOI is directly related to the atmospheric response during ENSO and so may prove to be a better predictor of Australian rainfall than are indices of sea surface temperature. The Equatorial Southern Oscillation Index, used here, is the standardized anomaly of the difference between the average mean sea level pressure over 80°W-130°W, 5°N-5°S and 90°E-140°E, 5°N-5°S (http://iridl.ldeo.columbia.edu/maproom/.ENSO/.Time_Series/Equatorial_SOI.html). The equatorial SOI is highly correlated with the traditional SOI for all seasons ($r = 0.65$ to 0.95). The regions over which the average MSLP is calculated are shown in Fig. 1, panel (g). The regression of the equatorial SOI onto MSLP in Fig. 1, panel (g), shows a high pressure anomaly in the eastern Pacific Ocean and a low pressure anomaly to the north of Australia in SON, associated with a positive equatorial SOI. The equatorial SOI better represents these regions of MSLP variation associated with the oscillation of SST anomalies in the Pacific Ocean, while the traditional SOI was historically limited to weather station locations.

The ENSO SST indices are a measure of the average SST anomalies in the east and central Pacific Ocean, which are regions of strong variability and amplitude during ENSO. The NINO3 index is a measure of the average SST anomaly in the main region of strong SST variability in the eastern Pacific (150°W-90°W, 5°N-5°S). The NINO3.4 is a measure of the average SST anomaly a little farther west (120°W-170°W, 5°N-5°S). The NINO3.4 region is typically the region for which global climate shows the strongest sensitivity. The NINO4 box is farther west still (150°W-160°E, 5°S-5°N) and captures SST variations on the eastern edge of the Pacific warm pool. The locations of these boxes are shown in Fig. 1, panels (b), (d) and (f). The tendency for some recent El Niño events to be more concentrated in the central Pacific Ocean is captured by the EMI, which is calculated from the average SST anomaly over 165°E-140°W, 10°S-10°N, minus half the average SST anomaly over 110°W-70°W, 15°S-5°N, and minus half the average SST anomaly over 125°E-145°E, 10°S-20°W. This is shown in Fig. 1, panel (c). A positive EMI is associated with warm SST anomalies in the central Pacific Ocean and cooler SST anomalies in the west Pacific Ocean and north of Australia. We note the EMI is essentially an index of the second EOF of tropical Pacific SST (e.g. Ashok et al. 2007) and as such is essentially uncorrelated with the NINO3 index because the NINO3 index is essentially an index of the first EOF of tropical Pacific SST. Australian rainfall, especially across the north of the country, is sensitive to Modoki El Niño (e.g. Wang and Hendon 2007).

The Indian Ocean East and West Poles indices are a measure of average SST anomalies in the south-east tropical Indian Ocean (90°E-110°E, 10°S-0°S) and tropical west Indian Ocean (50°E-70°E, 10°S-10°N). The DMI is the difference between the Indian Ocean Dipole West Pole Index (IODW) and the Indian Ocean Dipole East Pole Index (IODE; Saji et al. 1999). The location of these poles is shown in Fig. 1, panel (a). A positive Indian Ocean Dipole (IOD) event is associated with positive SST anomalies in the west Indian Ocean and negative SST anomalies in the east Indian Ocean. Southern Australian climate is particularly sensitive to SST variations associated with the IOD (e.g. Cai et al. 2010).

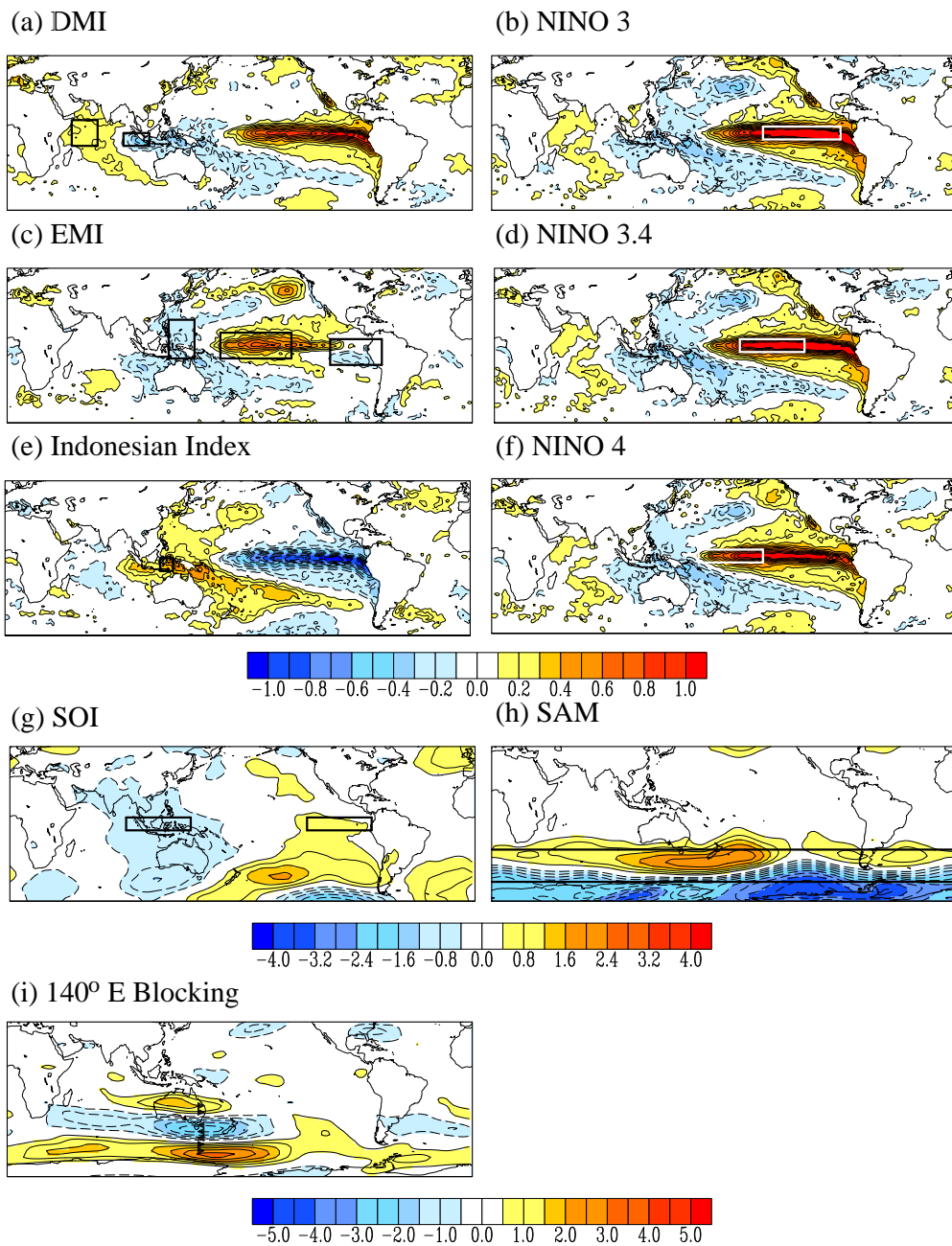


Fig. 1 Regression of observed index onto observed SST anomalies (panels (a) to (f)), observed MSLP anomalies (panels (g) and (h)), and observed 500hPa U wind anomalies (panel (i)) for SON. The black boxes in panel (a) show the locations of the Indian Ocean West and East Pole indices. The DMI is the difference between the SST anomalies in these regions. The white boxes in panels (b), (d) and (f) show the regions of the SST anomalies measured by the NINO indices. The black boxes in panel (c) show the three regions considered in the EMI index. The small black box to the north of Australia in panel (e) shows the location of the Indonesian Index region. The black boxes in panel (g) show the two regions over which the equatorial SOI is determined. SAM is the difference in the normalised monthly zonal MSLP at the latitudes indicated by the horizontal black lines in panel (h). The 140°E Blocking Index is the difference between the 500hPa zonal wind at the latitudes indicated by the black triangles in panel (i).

The SAM index is a measure of the difference in the normalised monthly zonal mean sea level pressure at 40°S and 65°S (see Fig. 1, panel (h); Marshall 2003) and monitors the north-south shift of the extratropical westerlies. High SAM is associated with a southward shift of the jet and an intensification of the polar vortex. High SAM is typically associated with easterly anomalies across extratropical Australia (e.g. Hendon et al. 2007). Compared to the ENSO indices, the timescale of the SAM index is much shorter and thus may not be a useful index for longer lead forecasts.

The 140°E Blocking Index is a measure of the zonal wind at 140°E and latitudes spanning 25°S-60°S (see Fig. 1, panel (i) for an illustration of the locations of the latitudes). The index is equal to $0.5(U_{25S} + U_{30S} - U_{40S} - 2U_{45S} - U_{50S} + U_{55S} + U_{60S})$. This index monitors the tendency for the typical west-east progression of weather systems to be “blocked” at the longitudes of eastern Australia (e.g., Risbey et al. 2009).

The Indonesian SST Index (Verdon and Franks 2005) is a measure of the average SST anomaly in a region north-west of Australia, in the south-east tropical Indian Ocean (120°-130°E, 10°-0°S); see Fig. 1, panel (e). Australian winter rainfall is sensitive to SST variations in this region.

4 PREDICTING INDICES WITH POAMA

Figures 2, 3 and 4 show the correlation of the predicted (POAMA versions p15b and p24) and observed indices for 1980-2006 at lead times of 0-2 months. Persistence is also included. The POAMA predicted ENSO indices are highly skilful (correlations >0.8) for lead times out to 2 months and beyond (e.g. Zhao and Hendon 2009). Of particular note is that the predictions from POAMA readily beat persistence during boreal spring (i.e. the model overcomes the spring persistence barrier).

The POAMA predictions of the IOD indices are strongly correlated with the observations in winter and spring ($r \sim 0.7 - 0.8$), although compared to the ENSO indices it is now more challenging to beat a persistence forecast. And, overall forecast skill in the Indian Ocean is lower than for the ENSO indices. Importantly, the IOD is not predictable at longer lead times (e.g. beyond 5 months, Zhao and Hendon 2009). Forecast skill for the Indonesian Index is similar to the IOD (strongest in spring).

Forecast skill for the SAM and the 140°E Blocking Index is relatively modest in comparison to the SST indices, reflecting that extratropical atmospheric variability is more difficult to forecast and is much less persistent than tropical SST. POAMA’s predictions for lead times 0-2 months of the 140°E Blocking Index mostly beat a persistence forecast in all seasons, while POAMA’s prediction of the SAM only consistently beats persistence in spring. Forecast skill for SAM and the 140°E Blocking Index also drops off more quickly with lead time than do the SST based indices and they are not predictable at lead times longer than 2 months.

In summary, forecast skill is highest for the Pacific Ocean SST indices (and the SOI), reflecting the long time scale of the coupled ocean-atmosphere variability there. The POAMA forecasts are able to overcome the boreal spring persistence barrier. The Indian Ocean SST indices are well predicted in winter and spring to a lead time of about 4-5 months. The SAM and 140°E Blocking indices have lower skill than the SST indices, reflecting the shorter timescales of these

phenomena. The POAMA forecasts of the atmospheric indices at lead times 0-2 months do, however, beat persistence.

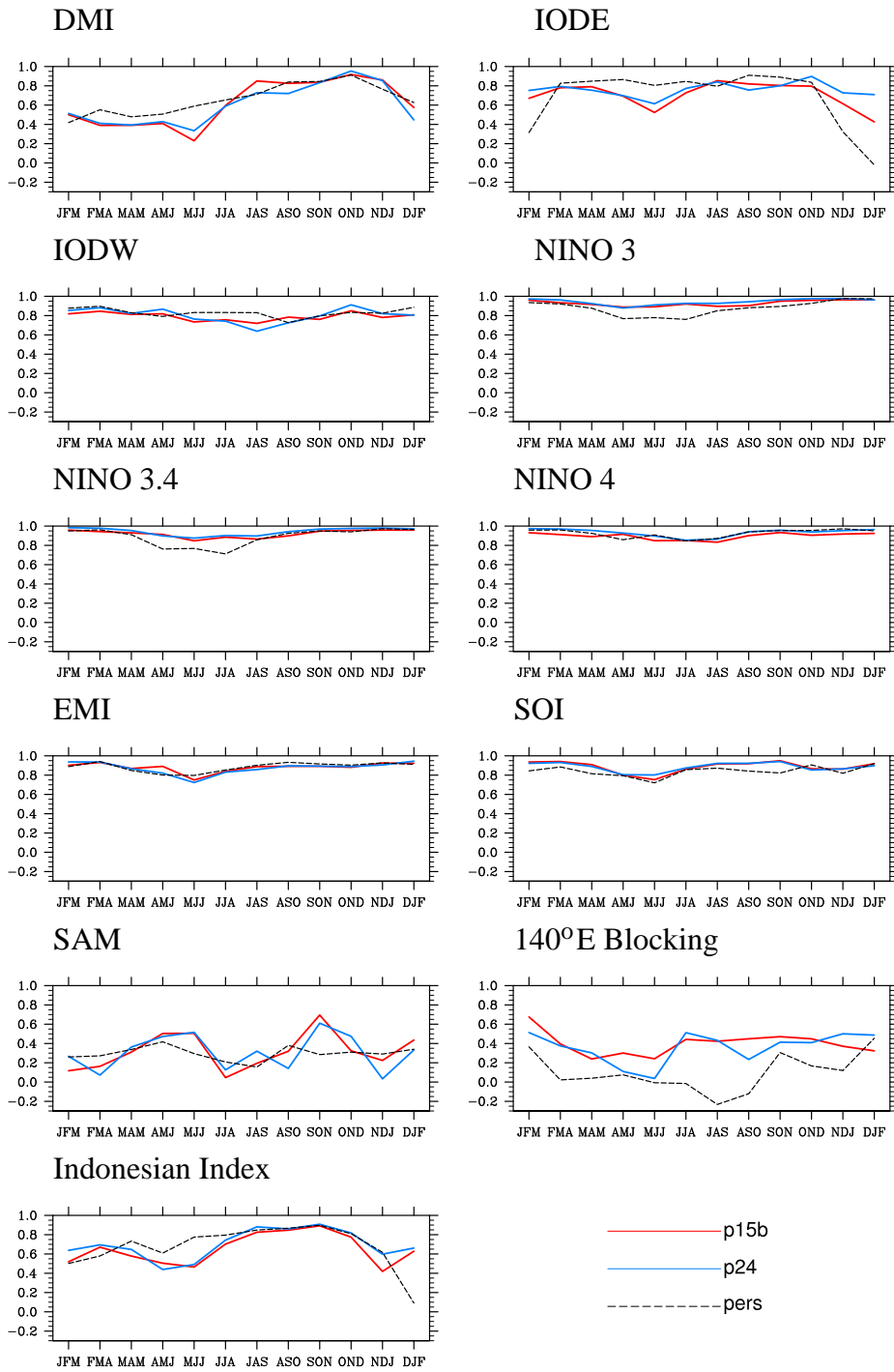


Fig. 2 Correlation of observed and predicted seasonal mean indices, for 1980-2006 and a lead time of 0 months. The season indicated on the x-axis is the verification season.

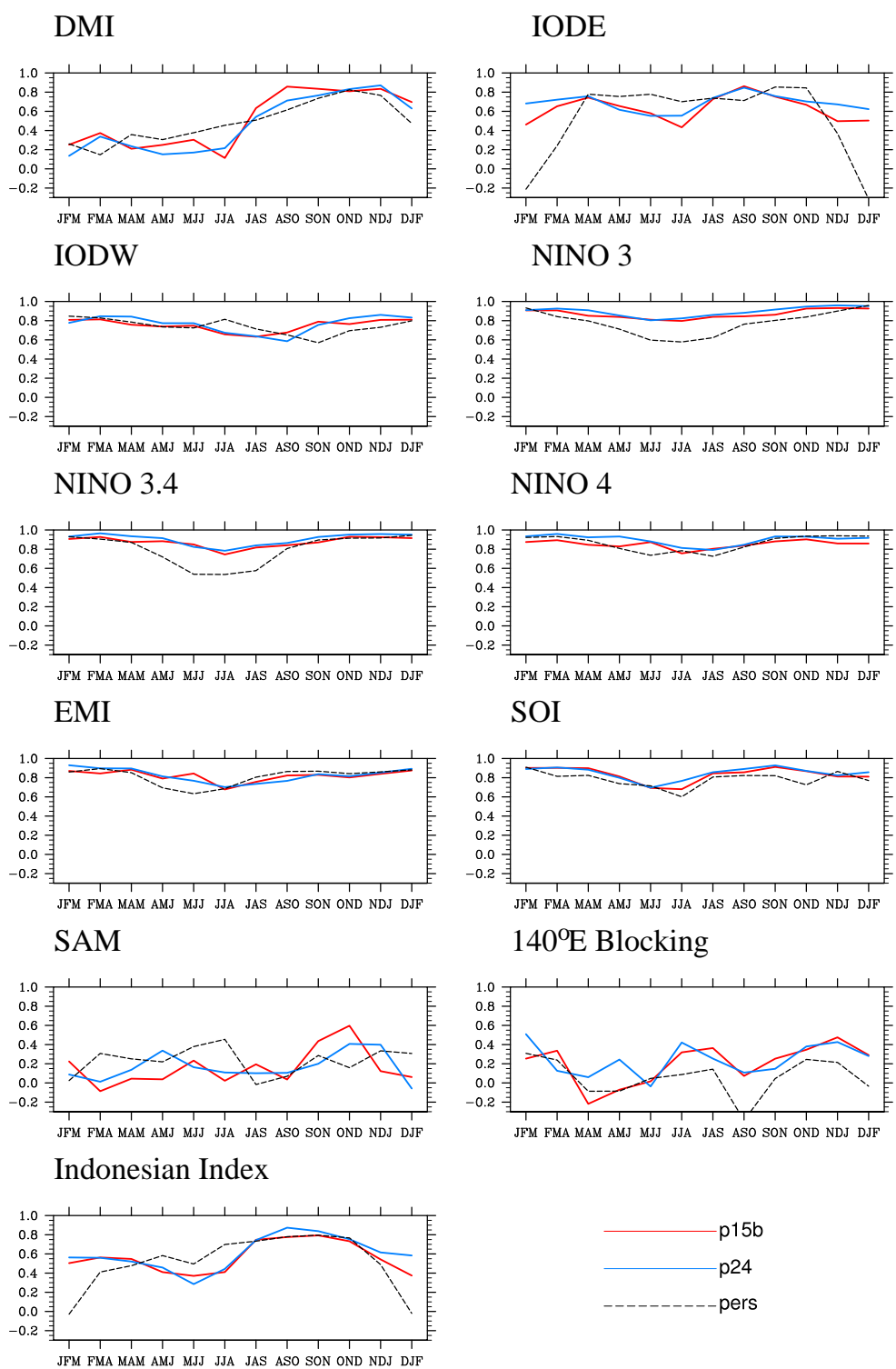


Fig. 3 Correlation of observed and predicted seasonal mean indices, for 1980-2006 and a lead time of 1 month. The season indicated on the x-axis is the verification season.

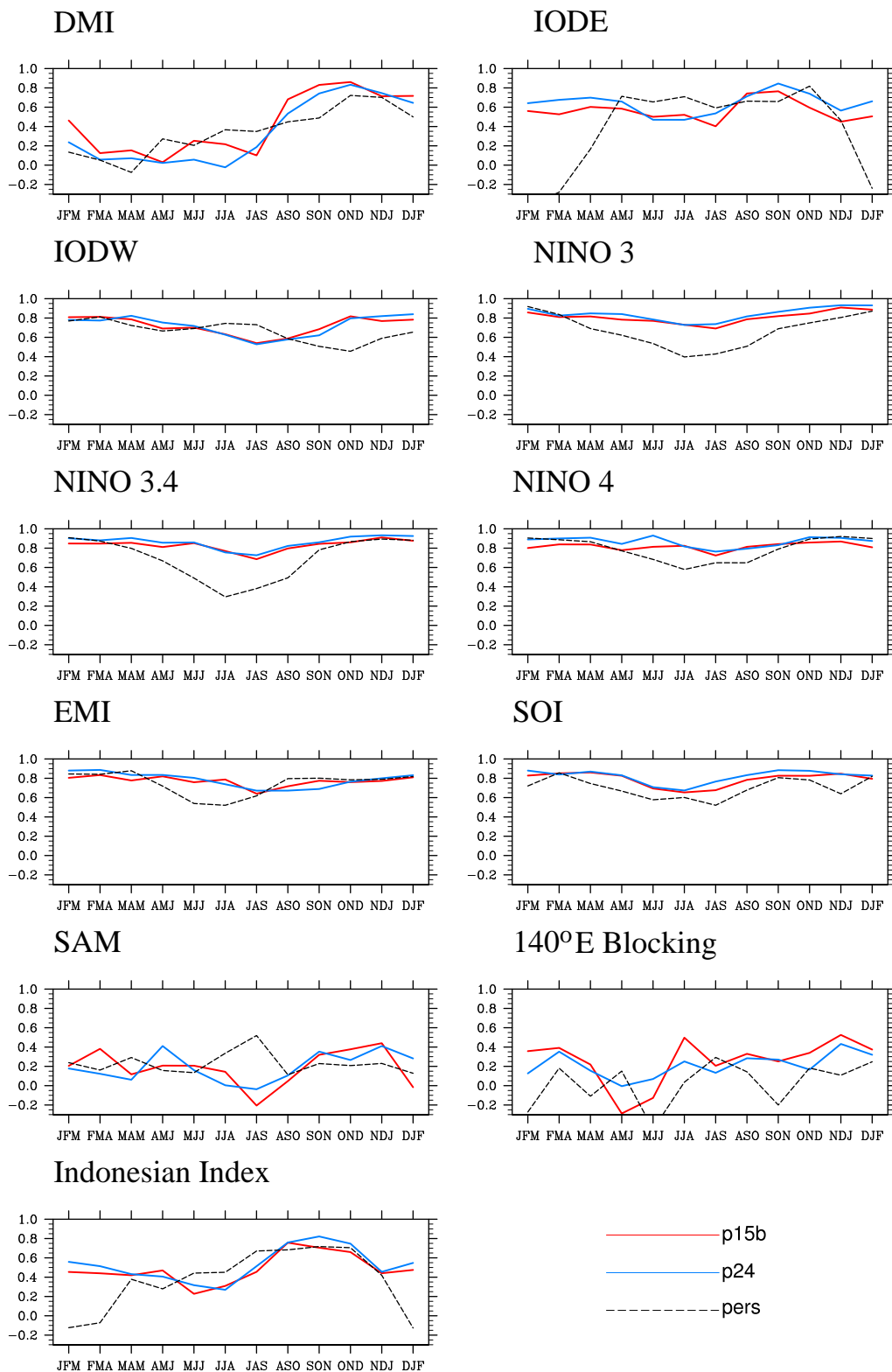


Fig. 4 Correlation of observed and predicted seasonal mean indices, for 1980-2006 and a lead time of 2 months. The season indicated on the x-axis is the verification season.

4.1 Relationship with rainfall

The ability to predict these climate indices will be of utility to the degree that they are related to rainfall variability. The relationship of these indices to Australian rainfall has previously been documented by Risbey et al. (2009). Here we review these relationships by regressing observed gridded rainfall onto the observed indices. This analysis is based on data for 1980-2006. The results are displayed as the regression coefficient at each grid point scaled for a one standard deviation anomaly of the index. The regression coefficient is therefore displayed in mm/day per standard deviation of the index anomaly. The regression maps for the standard seasons (MAM, JJA, SON and DJF) are displayed in Fig. 5. The maps for the complete set of 3-month means are displayed in the appendix (Figs A1-A4 in appendix A).

In autumn (Fig. 5), the standard ENSO SST indices (NINO3, NINO3.4, NINO4) show a negative regression coefficient with rainfall anomalies on the north-west coast. The EMI shows a stronger and broader relationship with rainfall, with significant anomalies in the central Northern Territory, and the central east coast. The DMI shows a strong relationship with rainfall along the east coast. The equatorial SOI and SAM indices have significant rainfall signals, but with the opposite sign to the ENSO SST indices, in the north-west. There is little association of rainfall with the Indonesian Index, the 140°E Blocking Index or the poles of the IOD during autumn.

In winter, the relationship of rainfall with ENSO is now mainly in the east, with the farther west Niño indices (NINO4 and EMI as compared to NINO3.4) having a stronger impact (e.g. Wang and Hendon 2007). The DMI is associated with rainfall in the south-east and south-west, with most of this impact arising from the east pole of the dipole. The Indonesian Index and the 140°E Blocking Index also have a strong relationship with rainfall in the south-east. The SAM relationship is modestly positive in the central-east portion of the country (positive rainfall with positive SAM) and there is evidence of a negative relationship on the Dividing Range in the south-east, consistent with Hendon et al. (2007).

In spring, the ENSO SST indices have a strong negative relationship with rainfall throughout the east, while the response in the south-east is weak for the EMI. The DMI also has a strong negative relationship with rainfall in the south-east and this now comes equally from the east and west poles of the dipole. The pattern for the DMI bears some semblance to that for the Niño Indices, which we address below. The SAM, Indonesian and 140°E Blocking indices also have a strong positive relationship with rainfall in the central east, east and south-east, respectively.

Due to the strong correlation between the ENSO and IOD indices in spring (Table 9), some of the association of rainfall with the DMI might stem from the co-variability with the ENSO SST indices. In order to separate out these signals, a multiple linear regression analysis is performed. We measure the amount by which the rainfall anomaly increases when one index is increased by a single standard deviation, and the other index is held constant. As an example, we show the partial regression analysis of the DMI and NINO3 (Fig. 6). The rainfall signal in the south-east associated with the DMI and NINO3 is seen to primarily stem from the association with the DMI. The rainfall variations further north is associated with the NINO3 index. The association for rainfall variations in the south with the DMI and in the north with NINO3 was explained physically by Cai et al. (2010; discussed below).

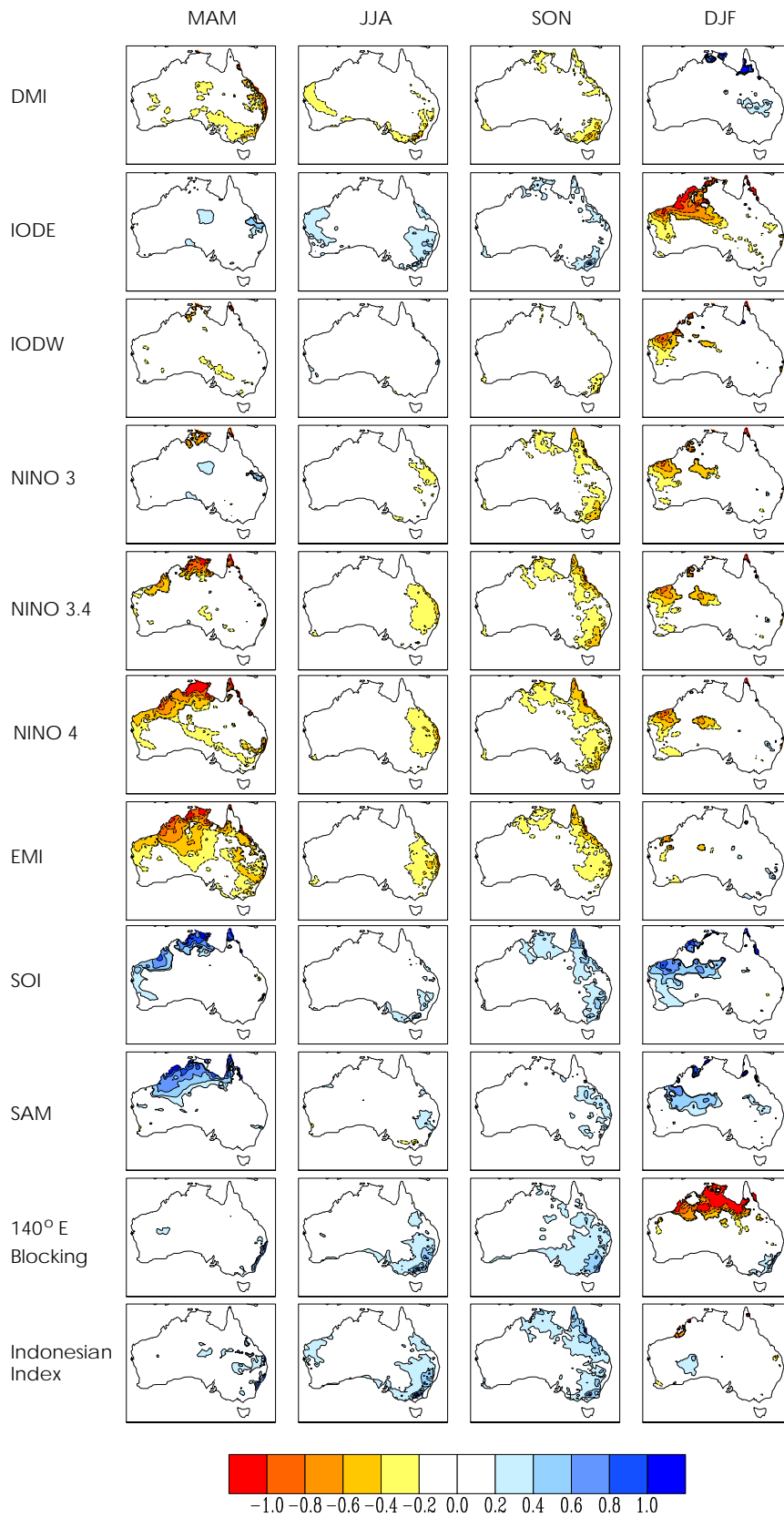


Fig. 5 Regression of observed index standardized anomalies onto observed rainfall anomalies for 1980-2006. Only regression coefficients with significance greater than 90 per cent are shown.

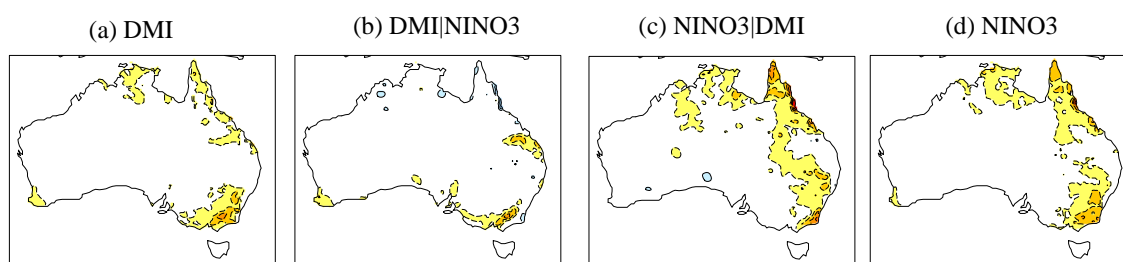


Fig. 6 (a) Regression of DMI index with rainfall anomalies. (b) Partial regression of DMI index with rainfall anomalies, with NINO3 contribution to co-variability removed. (c) Partial regression of NINO3 index with rainfall anomalies, with DMI contribution to co-variability removed. (d) Regression of NINO3 index with rainfall anomalies. All regression coefficients for SON, 1980-2006.

We also explore the co-variability of NINO3 and NINO4. The partial regression analysis for NINO3 and NINO4 is displayed in Fig. 7. We see that NINO4 has a stronger association with rainfall in the northern part of the continent, than does the more eastern Pacific Ocean NINO3 index. The south-east rainfall variations during ENSO are thus interpreted to mainly come via the co-variation of SST in the Indian Ocean because the NINO3 index is more highly correlated with the DMI index ($r = 0.78$) than is the NINO4 index ($r = 0.62$). Cai et al. (2010) interpret these results to indicate that the rainfall response across the south of Australia during El Niño or during an IOD event originates from SST variations in the eastern Indian Ocean, which excite eastward and poleward propagating atmospheric Rossby waves. These Rossby waves are equivalent barotropic and act to perturb the storm track across southern Australia. The rainfall response in the north eastern portion of the continent during El Niño originates from SST variations in the central Pacific and is interpreted as the steady tropical response to tropical heating (i.e. the generation of the Southern Oscillation; Gill 1980). This response has a baroclinic structure in the vertical and is trapped within 25 degrees of the equator.

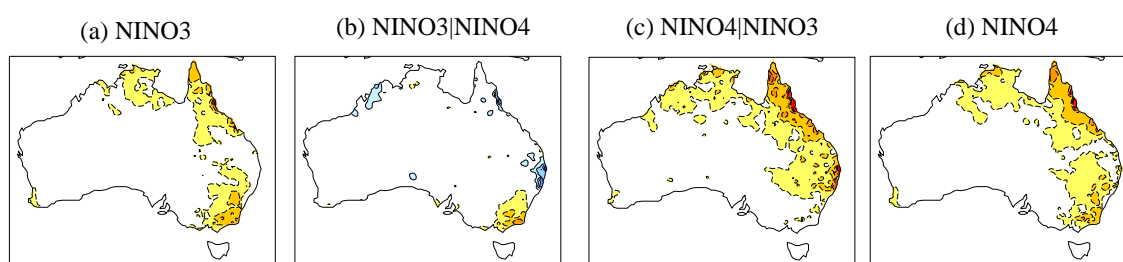


Fig. 7 (a) Regression of NINO3 index with rainfall anomalies. (b) Partial regression of NINO3 index with rainfall anomalies, with NINO4 contribution to co-variability removed. (c) Partial regression of NINO4 index with rainfall anomalies, with NINO3 contribution to co-variability removed. (d) Regression of NINO4 index with rainfall anomalies. All regression coefficients for SON, 1980-2006.

Returning to the association of the climate indices with rainfall, we see that in summer (Fig. 5), the regression coefficients have large magnitudes in the northern part of country, reflecting the seasonal increase of monsoonal rainfall to the north and west. Interestingly, rainfall in the north-west is now negatively correlated with SST in the eastern Indian Ocean, where as rainfall is still modestly negatively correlated with ENSO in the west, and positively correlated with SOI and SAM in this region. The 140°E Blocking index shows a strong negative signal in the north and the opposite sign in the south-east. The relationship of the 140°E Blocking Index with rainfall in

the north during summer needs further explanation. Note that the results for this assessment of the observed relationships are not cross validated.

4.2 Cross correlation of observed indices

In this section, the cross-correlation of the observed indices is further explored (Tables 1-12 in appendix A). High cross-correlation indicates indices that will exhibit similar co-variability with observed rainfall, and therefore yield similar predictions of Australian rainfall. This co-variability is also illustrated in Fig. 1 for SON.

The IODE has a strong negative correlation with the DMI; this peaks in spring ($r = -0.85$; Table 9) and then weakens over summer ($r = -0.13$; Table 12). This is similar for the positive correlation of DMI with the ENSO SST indices ($r = 0.62$ to 0.78 in SON; Table 9, $r = 0.30$ to 0.39 in DJF; Table 12). In the previous Section the co-variability of these indices with rainfall is seen to overlap in the south-east of Australia in SON, due to this correlation. In Fig. 1 panel (a) the regression of the DMI onto SST anomalies shows a strong relationship with the SST anomalies in the equatorial Pacific Ocean, in the same region as the NINO indices (see panels (b), (d) and (f) of Fig. 1). The individual poles of the DMI are correlated with the ENSO SST indices across summer and spring ($r \sim 0.6$ to 0.7 in DJF for both IOD poles; Table 12, $r \sim -0.5$ to -0.65 in SON; Table 9), but not autumn and winter. In summer the indices for IODE and IODW are also correlated with each other ($r = 0.75$ in JFM; Table 1). The IOD Pole indices are negatively correlated with the equatorial SOI ($r = -0.5$ to -0.6 ; Table 1, 12) in summer. In spring there is a positive correlation of the equatorial SOI with IODE ($r = 0.66$; Table 9), and a negative correlation with DMI and IODW ($r = -0.47$; Table 9).

The ENSO SST indices are highly correlated with each other for all seasons ($r = 0.66$ to 0.97). This can be seen in Fig. 1, panels (b), (d) and (f) for SON; the regression of the ENSO SST indices onto the SST anomalies shows a positive relationship in the overlapping regions in the equatorial western Pacific Ocean. The smaller correlation coefficients are for the NINO3 and NINO4 indices in autumn and winter. The ENSO SST indices are strongly anti-correlated with the equatorial SOI ($r = -0.69$ to -0.95), but the EMI is generally uncorrelated with the SOI, with the strongest negative correlation in JFM ($r = -0.54$; Table 1).

The Indonesian Index is correlated with IODE for all seasons ($r = 0.54$ to 0.86), and IODW in summer ($r \sim 0.6$; Table 1, 2). The Indonesian Index is negatively correlated with the DMI for all seasons, and the ENSO SST indices in winter and spring. It is also positively correlated with the equatorial SOI in winter and spring. The co-variability of the Indonesian Index with other SST indices can be seen for SON in Fig. 1, panel (e). The regression of the Indonesian Index onto SST anomalies shows a strong negative relationship in the NINO regions and the western Indian Ocean, and a positive relationship with the eastern Indian Ocean. The SST indices are thus the most likely to provide redundant or overlapping information about rainfall and some care should be used in deciding how many and which SST indices to include in any predictive scheme.

Based on this assessment of the cross-correlation of the indices, and based on the relationship of the indices with rainfall, we can tentatively recommend a sub set of the indices that could be used in a multi-predictor scheme: NINO3, EMI, DMI, 140°E Blocking Index, and SAM. The rationale for NINO3 and the EMI is that they are only weakly correlated but together they

capture the bulk of the ENSO related rainfall anomalies in Australia. The 140°E Blocking Index and SAM are probably only worthwhile at short lead times, but they provide independent information from the ENSO indices. Choice of the DMI over the IODE or the Indonesian Index is subjective, but the DMI does have the strongest associations with rainfall in the seasons other than SON (when the IOD tends to peak).

5 ASSESSMENT OF SKILL

In this Section, we assess the skill of making rainfall predictions using the predicted indices from POAMA. The results were cross-validated for 1980-2006. This means that method was repeated, leaving out a single independent year at a time, in order to fairly assess the skill for predicting the seasonal Australian rainfall. The standardized anomalies of the POAMA predicted indices were calculated for the subset of the years. The relationship with the observed rainfall anomalies in the same subset of years was determined from a regression analysis. The standardized anomaly for the predicted index from POAMA in the independent year was determined using the climatology of the subset of years. This was then used to predict the rainfall anomaly for the independent year based on the observed relationship between the index and rainfall developed in the subset of years.

In order to assess skill of the rainfall predictions for 1980-2006, the root mean square error (RMSE) was calculated. See Section 1 for a description of this method of forecast verification. The RMSE skill score was then calculated with climatology as the reference forecast.

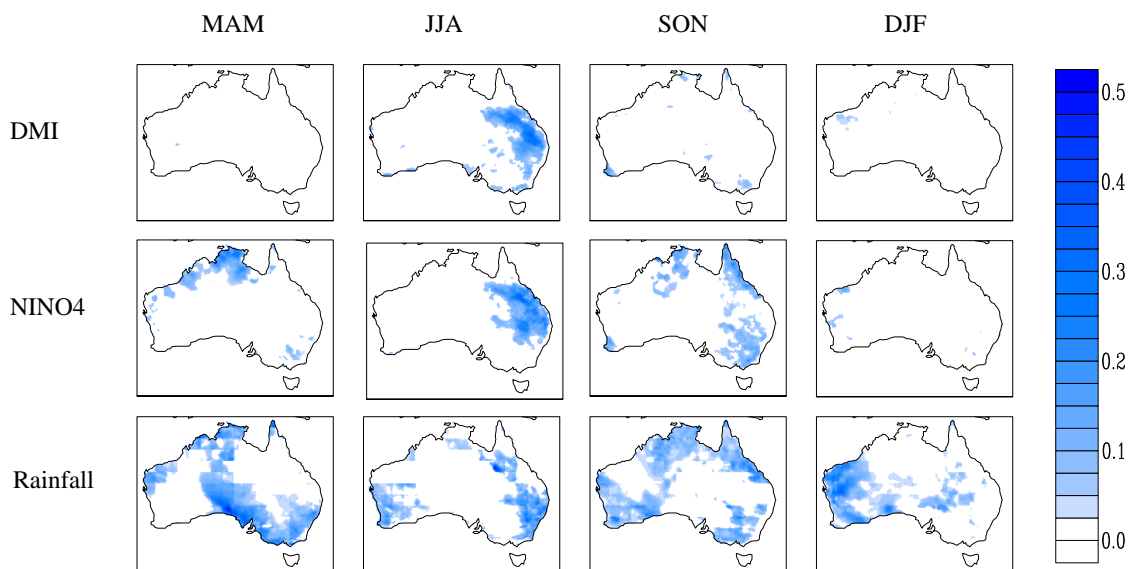


Fig. 8 RMSE skill score for predicting Australian rainfall with POAMA version p15b, compared to climatology for lead time 0 months. Results shown for DMI and NINO4 indices and the POAMA direct rainfall forecast. 1980-2006.

An example of the RMSE skill score is shown in Fig. 8 for lead time 0 months using POAMA version p15b. The results are shown for rainfall predicted using the DMI and NINO4 indices and the direct output of rainfall from POAMA, all compared to a climatological forecast. The darker blue regions indicate regions where the predictions show higher skill compared to forecasting climatological rainfall. A perfect forecast would have a RMSE value of zero, and

hence a RMSE skill score of 1. White indicates that climatology is a more skilful indicator of the rainfall anomalies in that region. For the regions where the significance of the regression coefficient used to predict the rainfall anomaly based on the climate indices was less than 90 per cent, the RMSE is set to the variance of the observed rainfall anomaly. This means that the skill score for that index will be zero, if all the regressions for the cross validated years are not significant. This indicates that the historical relationship of the index anomalies with the rainfall anomalies is not useful in skilfully predicting the Australian rainfall anomalies in the future.

In MAM there is some skill for NINO4 in predicting rainfall anomalies in the northwest. In Fig. 8 areas of skilful prediction of rainfall anomalies using the indices are seen in the east in JJA for both indices, extending further south for the DMI. In SON, skilful prediction of rainfall with NINO4 is seen in the north and east with the DMI having skill in the far south-west and south-east. There is an overlap of the skilful regions in the south-east for the DMI and NINO4 index, which is most likely due to the high correlation of these indices in this season, as discussed in Section 2. In comparison to the direct output from POAMA, these two indices have better skill in parts of the east during winter and spring. POAMA, on the other hand, has better skill in large parts of the country in autumn and in the west during winter, spring and summer.

The complete set of RMSE skill scores for all indices and all months and for lead times 0, 1 and 2 months and for both versions of POAMA are displayed in the appendix, Figs A5-A28 in appendix A. In autumn the ENSO indices show skill for predicting rainfall anomalies in the north. In winter, the ENSO indices show highly skilful regions in the central east. The more central Pacific Ocean indices show skill further south. In spring, all ENSO indices show skilful regions in the south-east, the north and in the south-west of Western Australia. At the end of spring, the central Pacific Ocean indices also show skill in the central west. In summer the ENSO indices provide skilful predictions in the west of the continent.

The IOD indices show little or no skill in predicting Australian rainfall anomalies in summer and autumn. In winter, the DMI shows skill in predicting rainfall anomalies in the east, extending further south than the region of skill seen with the ENSO indices in this season. At the start of spring, the region of skill extends north for the DMI and the IODE, as the ENSO indices become more highly correlated with this index. After spring there are also regions of skill in the south-east for the DMI and IODW.

The SAM index shows little skill, a notable region is the north of Queensland in JFM, and the skill decreases rapidly with lead time. There are also patches of skill in the east in winter and the north in spring at longer lead times, which are not in regions where rainfall is typically associated with the SAM index (see Fig. 5). This was expected, due to the low correlation of the predicted indices with the observed indices (see Figs 2-4). The 140°E Blocking Index shows skill in predicting rainfall anomalies in the south-east in some seasons. This is not maintained with lead time, due to the uncertainty in predicting this index on seasonal time scales. The Indonesian Index shows skill in predicting rainfall anomalies in the north of the continent in spring.

5.1 Maximum skill plots

In order to summarize which index may be of most value to predict rainfall, we have constructed maps indicating the index (or POAMA) that has the highest RMSE skill score for

predicting the rainfall anomaly at each grid point, following the method of display by Risbey et al. (2009). Examples are shown in Figs 9 and 10 for POAMA version p15b and p24 for the standard seasons at lead time 0. Yellow areas in Figs 9 and 10 correspond to the POAMA rainfall forecast having the highest RMSE skill score relative to a climatological forecast. Blue areas correspond to the ENSO SST indices having the highest RMSE skill scores. Green colours indicate the Indian Ocean indices. The purple colours are associated with the 140°E Blocking Index, SAM and the Indonesian Index. We also include persistence (red).

In autumn (upper left of Figs 9 and 10), the direct output from POAMA has the single highest skill score for most of the country. On the other hand, the ENSO indices have the potential to improve the forecast over that directly from POAMA in large parts of the east in winter. In spring, POAMA dominates the highest skill in the west, while in the east there is a mishmash of highest skill from the ENSO indices, the Indian Ocean indices, the 140°E Blocking Index and the Indonesian Index. In summer, the Indian Ocean indices and POAMA provide the highest level of skill in the west. Interestingly, persistence also shows up in portions of eastern Western Australia. The RMSE skill score associated with the predictor that has the highest skill score at each grid point is displayed in Figs 11 and 12. Compared to what is directly provided by POAMA (bottom row of Fig. 8), the indices have the potential to improve the forecasts in large portions of the east during winter and spring, and in the west during summer. The complete set of maps of highest skill score are displayed in the appendix for lead times 0, 1, and 2 months, Figs A29-A30 in appendix A.

A point of caution is needed here. The plots in Figs 9-12 indicate the index that has the highest RMSE skill score and the RMSE skill score achieved from using just that index (or POAMA). What is not shown in Figs 9-12 is the RMSE skill score achieved if multiple indices are used. In order to make that calculation, a multiple regression is required, which is beyond the scope of the present study (the main goal here was to provide an assessment of potential candidate indices that could be used as predictors). However, if a multiple regression were to be constructed, then the number of indices should be reduced to avoid redundancy. As per the recommendation above, we have constructed a plot of the most skilful predictors based on the subset using the DMI, NINO3, the EMI, SAM, the blocking index and POAMA directly for lead time 0 month (Fig. 13). 140°E Blocking Index now figures prominently in the south-east during autumn and spring, where as the EMI is prominent in the east during winter and in the north-east during spring. The regions where POAMA rainfall is the best predictor are the same as when the full set of indices are used. The more spatially coherent regions of highest skill in Fig. 13 indicate the benefit of using a smaller selection of predictors that are less cross-correlated.

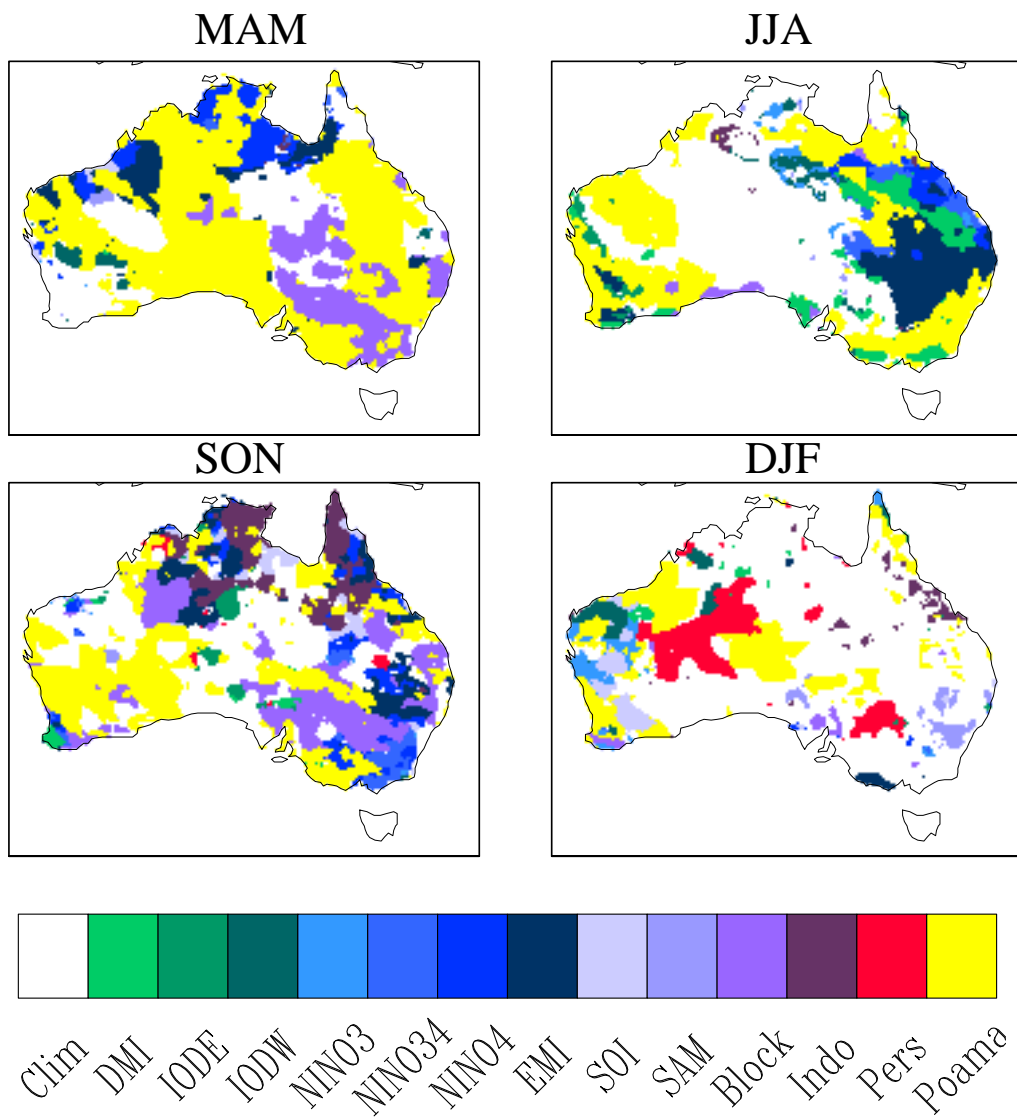


Fig. 9 Colours indicate the index with the highest RMSE skill score, for POAMA model version p15b compared to climatology, at lead time 0 months. 'Clim' refers to no index having a smaller RMSE than forecast by climatology. 'Pers' refers to persistence having the highest RMSE skill score. 'Poama' refers to the POAMA rainfall anomaly forecast having the highest RMSE skill score.

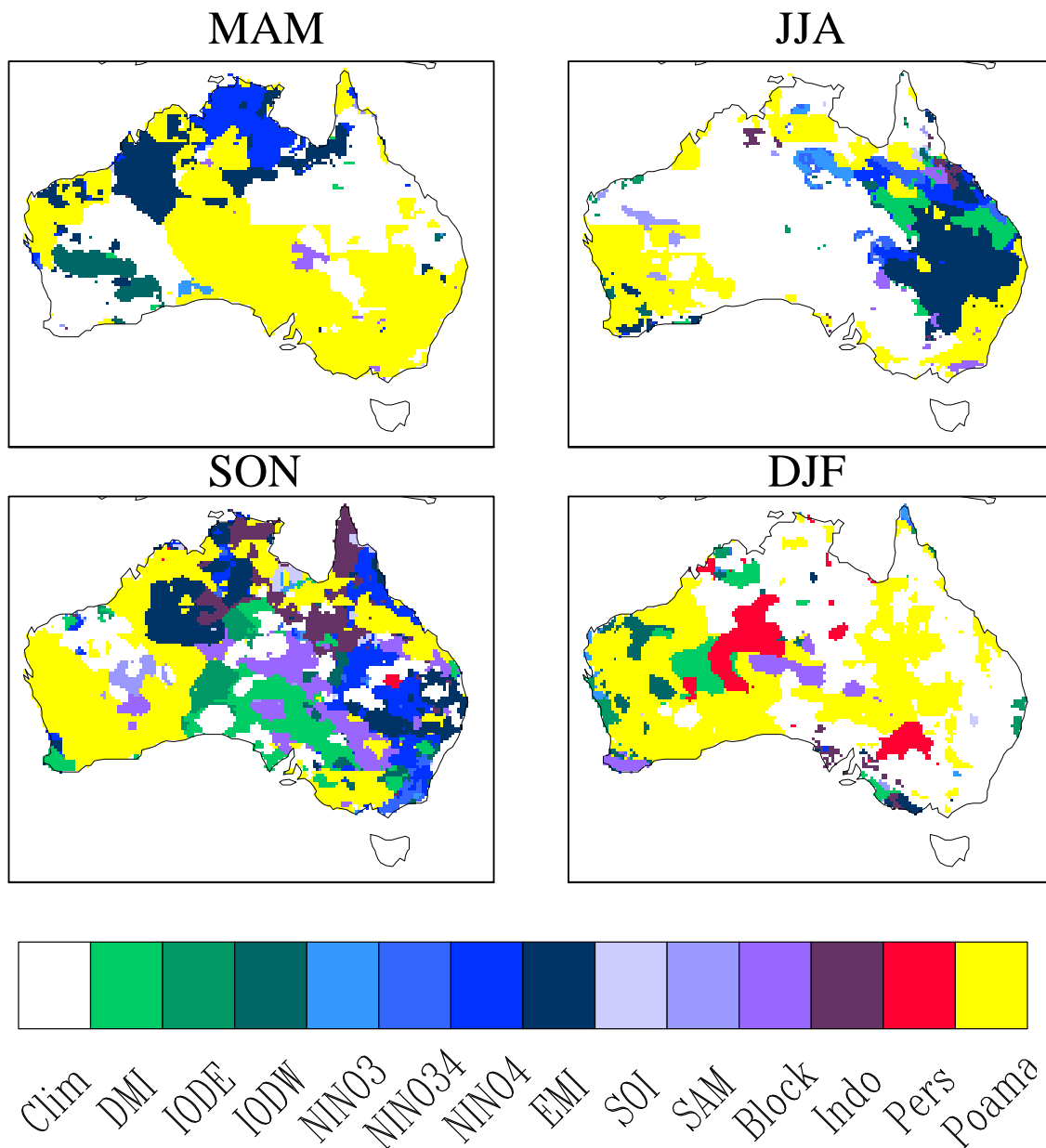


Fig. 10 Colours indicate the index with the highest RMSE skill score, for POAMA model version p24 compared to climatology, at lead time 0 months. 'Clim' refers to no index having a smaller RMSE than forecast by climatology. 'Pers' refers to persistence having the highest RMSE skill score. 'Poama' refers to the POAMA rainfall anomaly forecast having the highest RMSE skill score.

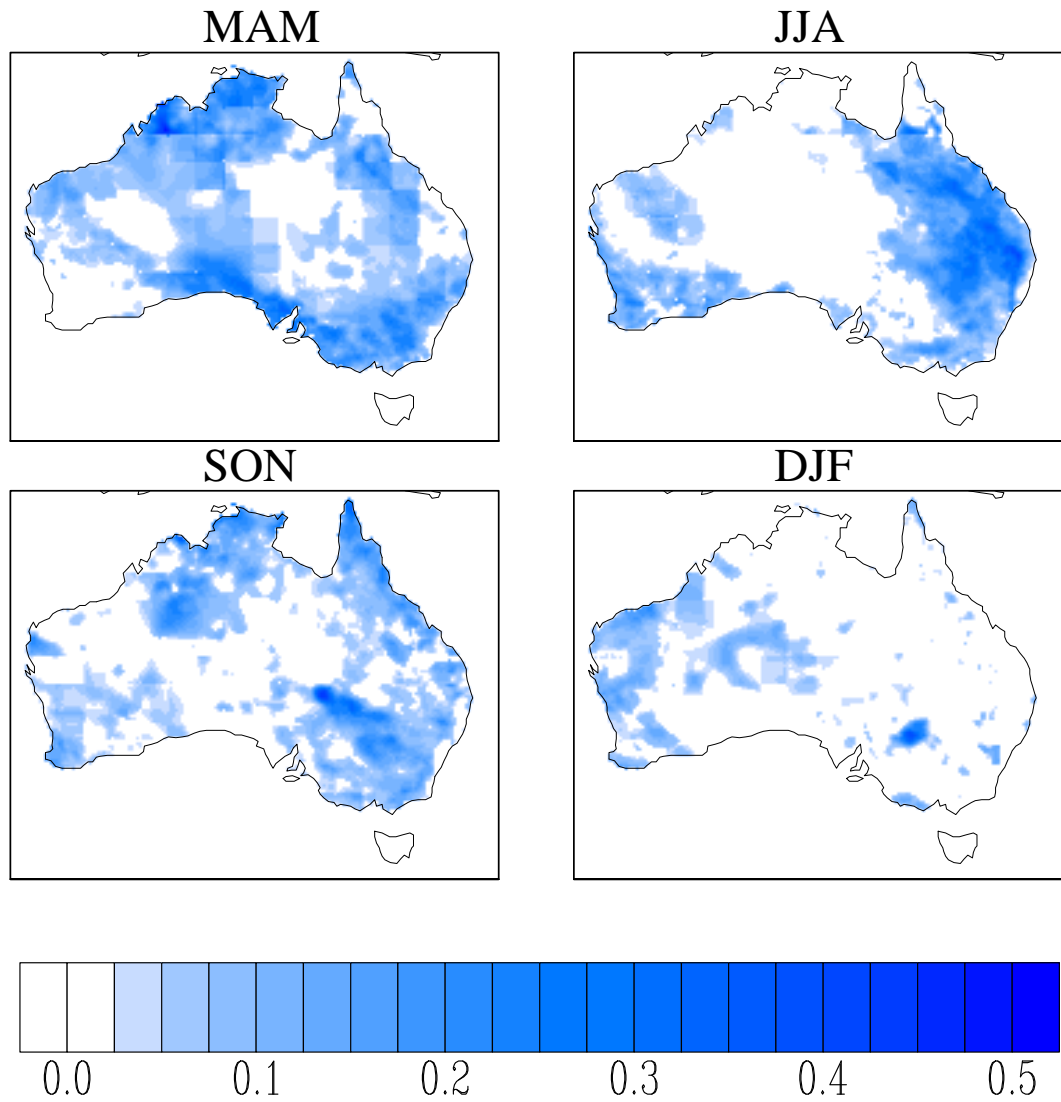


Fig. 11 The RMSE skill score corresponding to Fig. 9 - the highest RMSE skill score for all indices, climatology, persistence and POAMA forecasts. For POAMA model version p15b compared to climatology, at lead time 0 months.

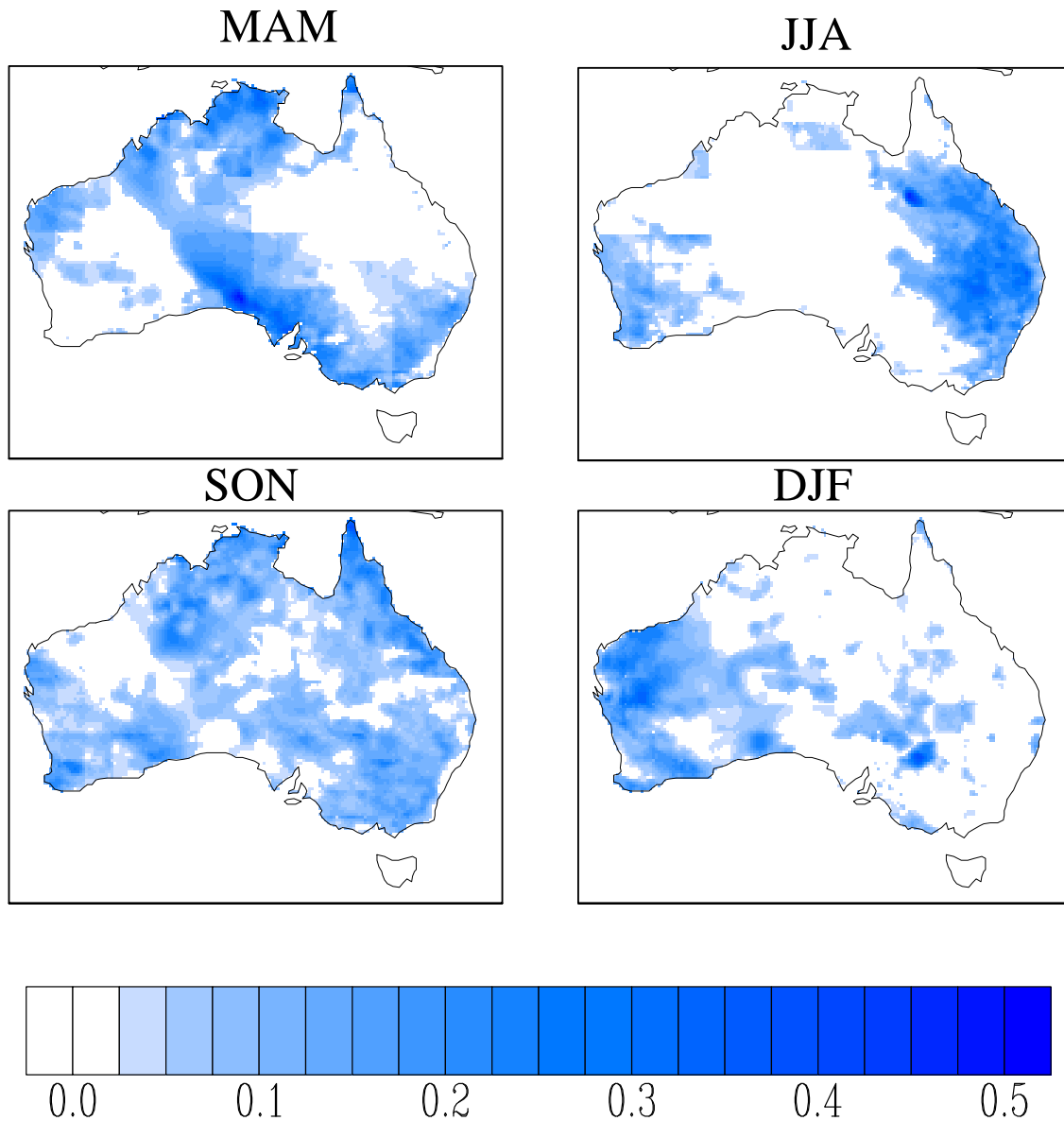


Fig. 12 The RMSE skill score corresponding to Fig. 10 - the highest RMSE skill score for all indices, climatology, persistence and POAMA forecasts. For POAMA model p24 compared to climatology, at lead time 0 months.

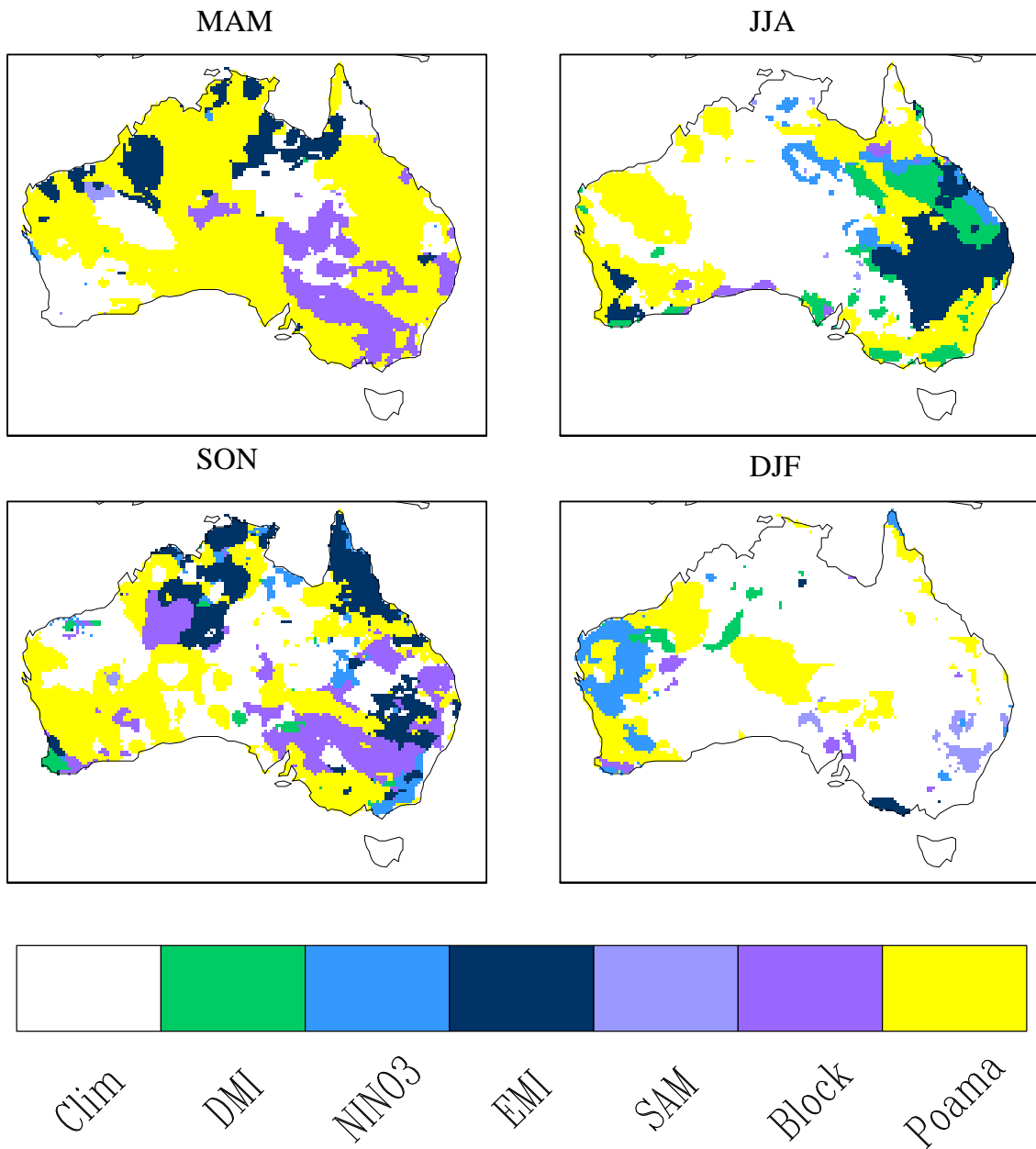


Fig. 13 Prediction of Australian rainfall with highest RMSE skill score, compared to climatology, as in Fig. 10, but for a select number of indices. Results for POAMA model version p15b, 1980-2006, lead time 0 months.

6 CONCLUSION

This study has assessed the possibility of using predictions of standard climate indices as possible predictors of Australian rainfall. These results suggest that there could be a significant benefit of using the predictions of the climate indices to provide better rainfall forecasts than are directly available from POAMA, especially at longer lead times. At longer lead times (4-9 months) the most skilfully predicted indices will be those associated with ENSO. Prediction of the IOD indices will be primarily useful only to a lead of ~ 4-5 months. The indices associated with atmospheric variability (140°E Blocking Index and SAM) will not be useful at lead times longer than 1-2 months.

Based on the ability to predict these indices and due to their relationship with Australian rainfall, we have demonstrated the possibility of improving the predictions of rainfall from POAMA by using the predicted indices as input predictors. For lead times to 2 months, we have shown additional benefit could be achieved from using a standard ENSO index (e.g. NINO3), the Modoki El Niño Index, the Dipole Mode Index, and 140°E Blocking Index and SAM. At longer lead times, the ENSO indices will be of most use because the IOD is not predictable beyond 4-5 months and the 140°E Blocking Index and SAM are not predictable beyond 1-2 months.

The results shown here do not take into account the additive predictability that could be obtained using multiple predictors. In this sense, the skill scores displayed for instance in Figs 11 and 12 can be considered a lower bound on what might be achievable. The method to combine predictors into a single rainfall prediction scheme needs to take into account the covariance of the predictors (e.g., multiple linear regression) and will need proper cross validation to avoid artificial skill. Previous experience with combining multiple predictors (e.g. Lim et al. 2010) indicates the both the predictive indices and the direct prediction of rainfall from POAMA should be used.

REFERENCES

- Cai, W., van Rensch, P., Cowan, T. and Hendon, H.H. (2010). Teleconnection pathways of ENSO and the IOD and the mechanisms for impacts on Australian rainfall. *J. Climate* (accepted).
- Hendon, H.H., Thompson, D.W.J. and Wheeler, M.C. (2007). Australian rainfall and surface temperature variations associated with the Southern Hemisphere annular mode. *J. Climate*, 20, 2452-2467.
- Hudson, D., Alves, O., Hendon, H.H. and Wang, G. (2011). The impact of atmospheric initialisation on seasonal prediction of tropical Pacific SST. *Clim. Dyn.* 36, 1155-1171.
- Jones, D.A. and Weymouth, G. (1997). An Australian monthly rainfall dataset. *Technical Report 70*, Bureau of Meteorology.
- Kalnay, E., Kanamitsu, M., Kistler, R., Collins, W., Deaven, D., Gandin, L., Iredell, M., Saha, S., White, G., Woollen, J., Zhu, Y., Leetmaa, A., Reynolds, R., Chelliah, M., Ebisuzaki, W., Higgins, W., Janowiak, J., Mo, K.C., Ropelewski, C., Wang, J., Jenne, R. and Joseph, D. (1996). The NCEP-NCAR 40-year reanalysis project. *Bull. Amer. Meteor. Soc.*, 77, 437-471.
- Lim, E.-P., Hendon, H.H., Hudson, D., Wang, G. and Alves, O. (2009). Dynamical forecast of inter-El Nino variations of tropical SST and Australian spring rainfall. *Monthly Weather Review*, 137, 3796-3810.
- Lim, E.-P., Hendon, H.H., Anderson, D.L.T., Charles, A. and Alves, O. (2010). Dynamical, statistical-dynamical and multi-model ensemble forecasts of Australian spring season rainfall. *Monthly Weather Review*, (In press).
- Marshall, G.J. (2003). Trends in the Southern Annular Mode from observations and reanalysis. *J. Climate*, 16, 4134-4143.
- Rayner, N.A., Parker, D.E., Horton, E.B., Folland, C.K., Alexander, L.V., Rowell, D.P., Kent, E.C. and Kaplan, A. (2003). Global analysis of sea surface temperature, sea ice, and night marine air temperature since the late nineteenth century. *J. Geophys. Res.*, 108, 4407.
- Risbey, J.S., Pook, M.J., McIntosh, P.C., Wheeler M.C. and Hendon, H.H. (2009). On the remote drivers of rainfall variability in Australia. *Monthly Weather Review*, 137, 3233-3253.
- Saji, N.H., Goswami, B.N., Vinayachandran, P.N. and Yamagata, T. (1999). A dipole mode in the tropical Indian Ocean, *Nature*, 401, 360-363.
- Smith, N.R., Blomley, J.E. and Meyers, G. (1991). A univariate statistical interpolation scheme for subsurface thermal analyses in the tropical oceans. *Progress In Oceanography*, 28, 219-256.
- Troup, A.J. (1965). The 'southern oscillation.' *Quarterly Journal of the Royal Meteorological Society*, 91, 490-506.

Verdon, D.C. and Franks, S.W. (2005). Indian Ocean sea surface temperature variability and winter rainfall: Eastern Australia. *Water Resources Research*, 41, W09413.

Wang, G., and Hendon, H.H. (2007). Sensitivity of Australian rainfall to inter-El Nino variations. *J. Climate*, 20, 4211-4226.

Yin Y., Alves, O. and Oke, P.R. (2010). An ensemble ocean data assimilation system for seasonal prediction. Submitted to *Monthly Weather Review*.

Zhao, M., and Hendon, H.H. (2009). Representation and prediction for the Indian Ocean dipole in the POAMA seasonal forecast model. *Quarterly Journal of the Royal Meteorological Society*, 135, 337-352.

APPENDIX - A

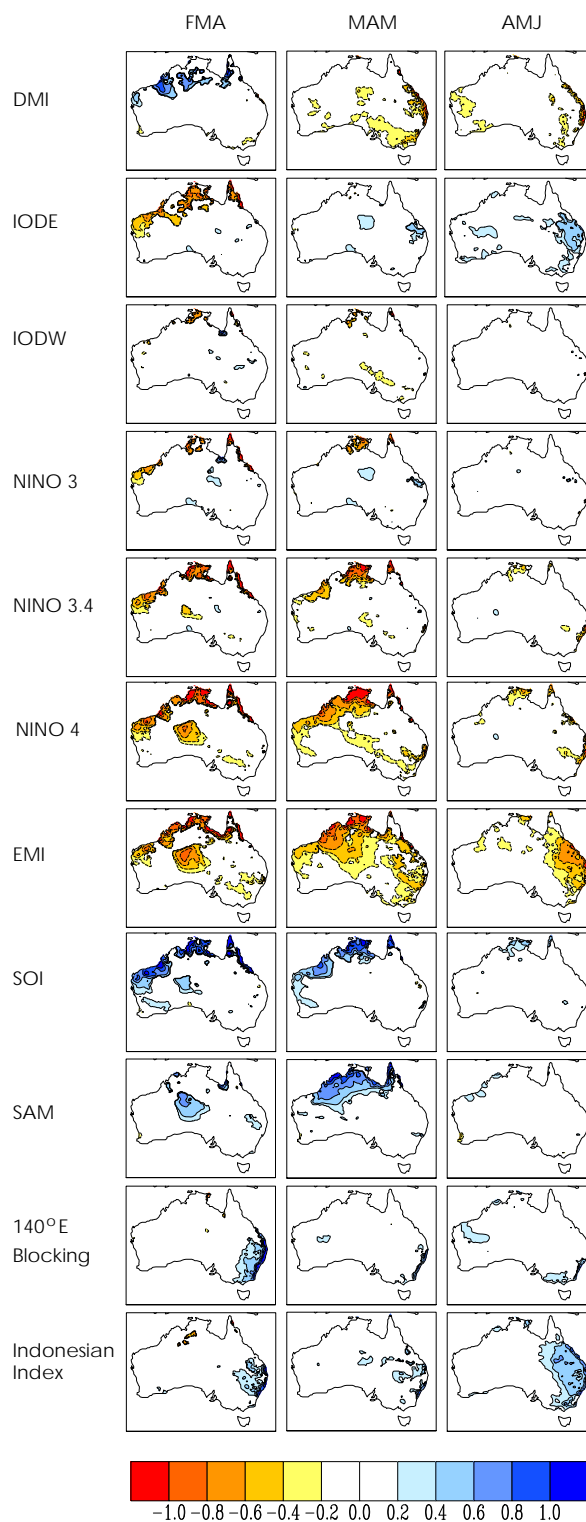


Fig. A.1 Autumn, regression of standardized anomalies of the observed indices onto observed rainfall anomalies for 1980-2006. Only regression coefficients with significance greater than 90 per cent are shown.

APPENDIX A

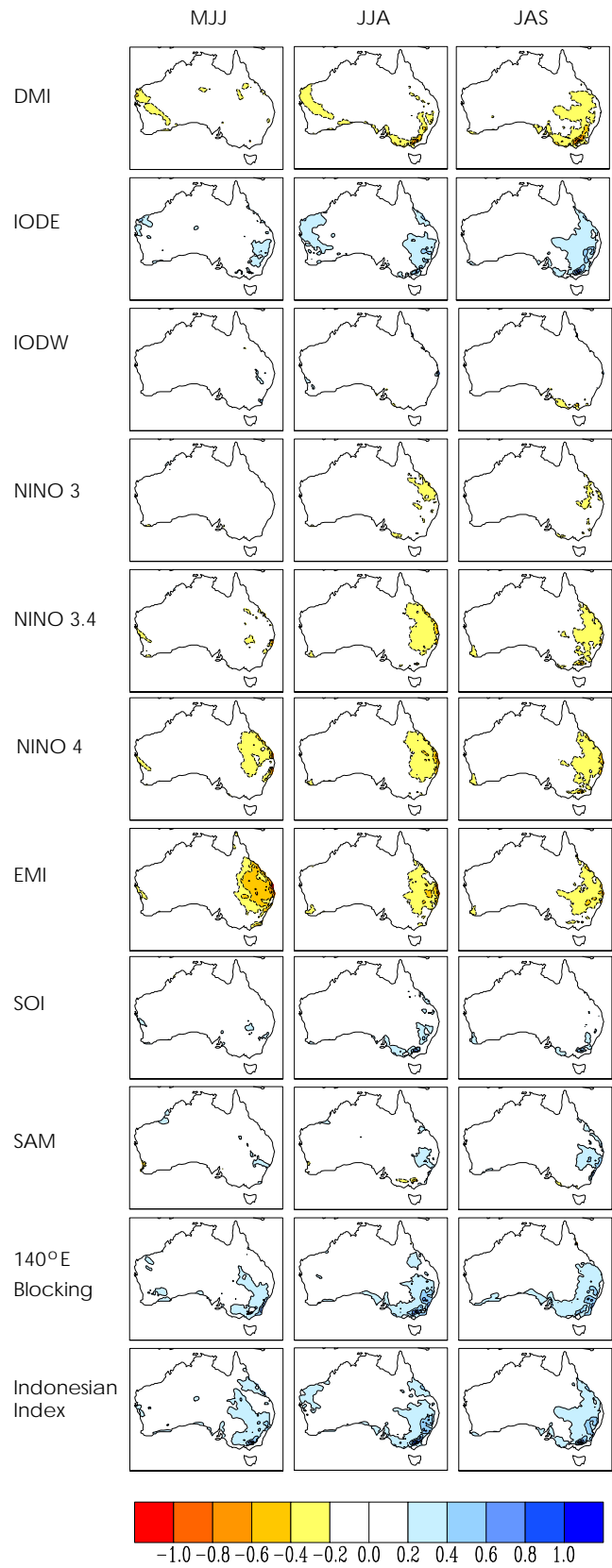


Fig. A.2 Winter, regression of standardized anomalies of the observed indices onto observed rainfall anomalies for 1980-2006. Only regression coefficients with significance greater than 90 per cent are shown.

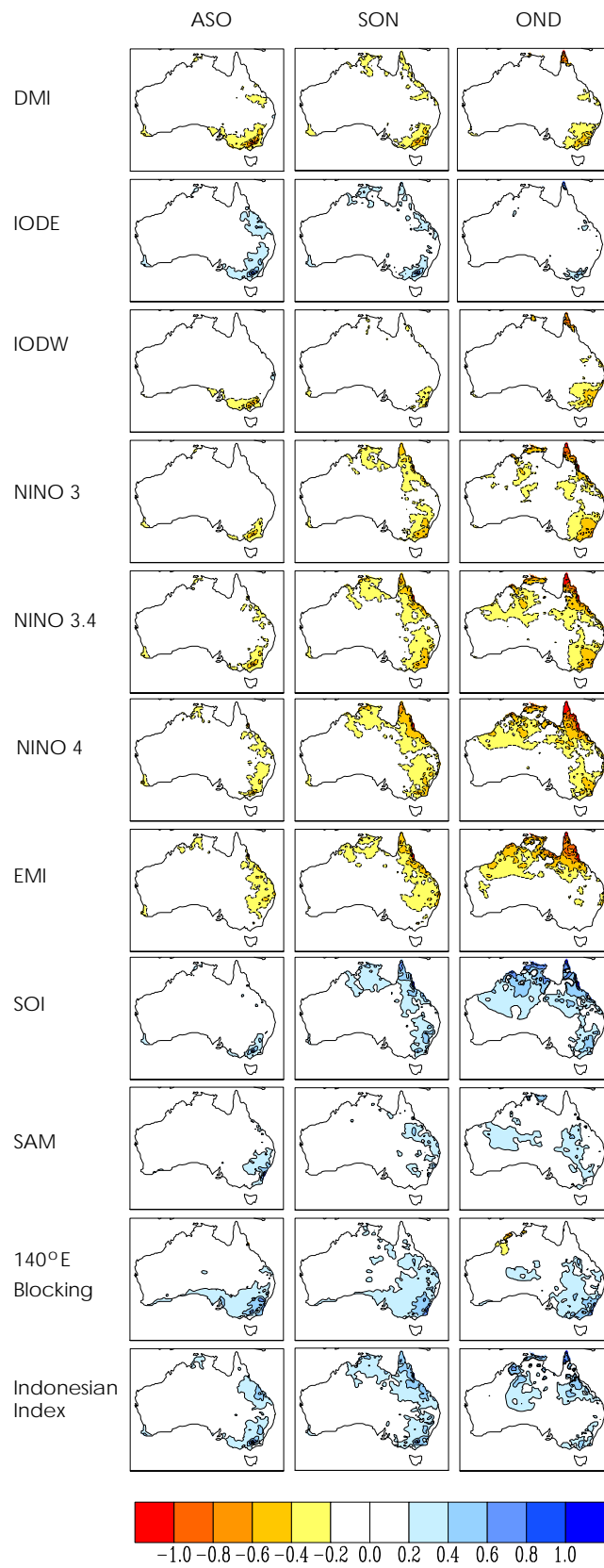


Fig. A.3 Spring, regression of standardized anomalies of the observed indices onto observed rainfall anomalies for 1980-2006. Only regression coefficients with significance greater than 90 per cent are shown.

APPENDIX A

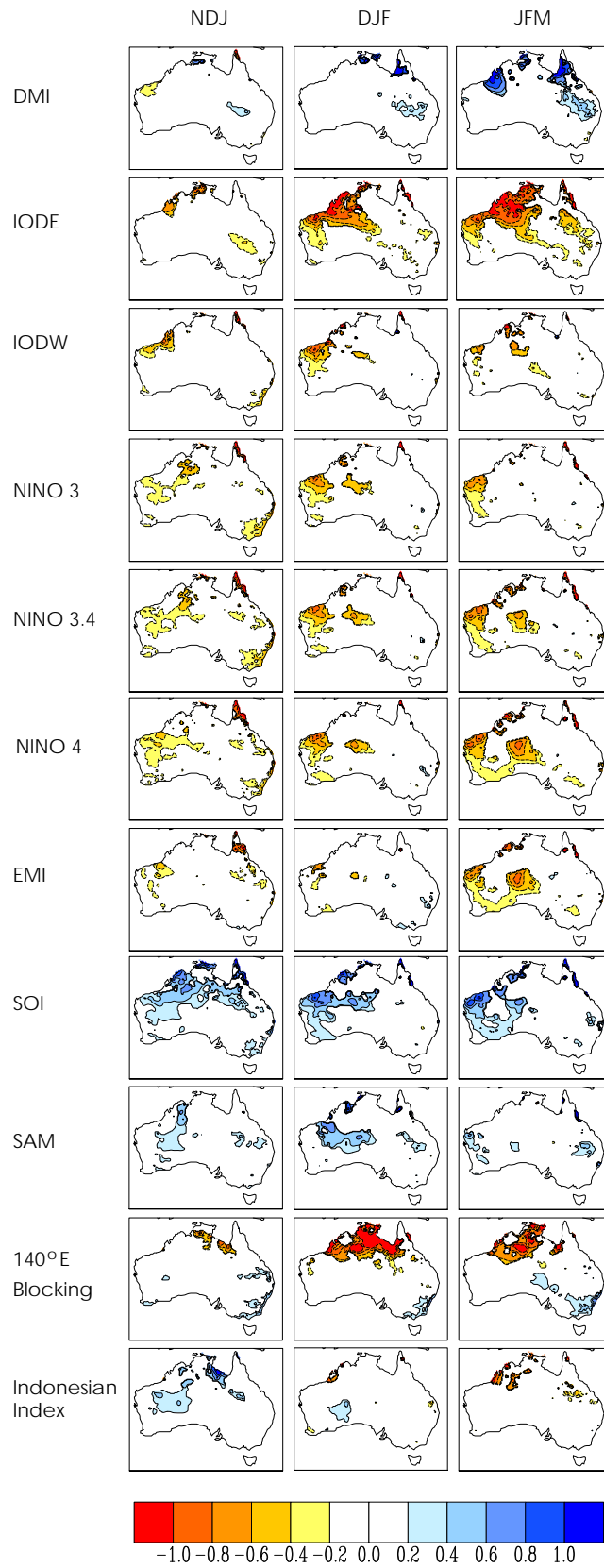


Fig. A.4 Summer, regression of standardized anomalies of the observed indices onto observed rainfall anomalies for 1980-2006. Only regression coefficients with significance greater than 90 per cent are shown.

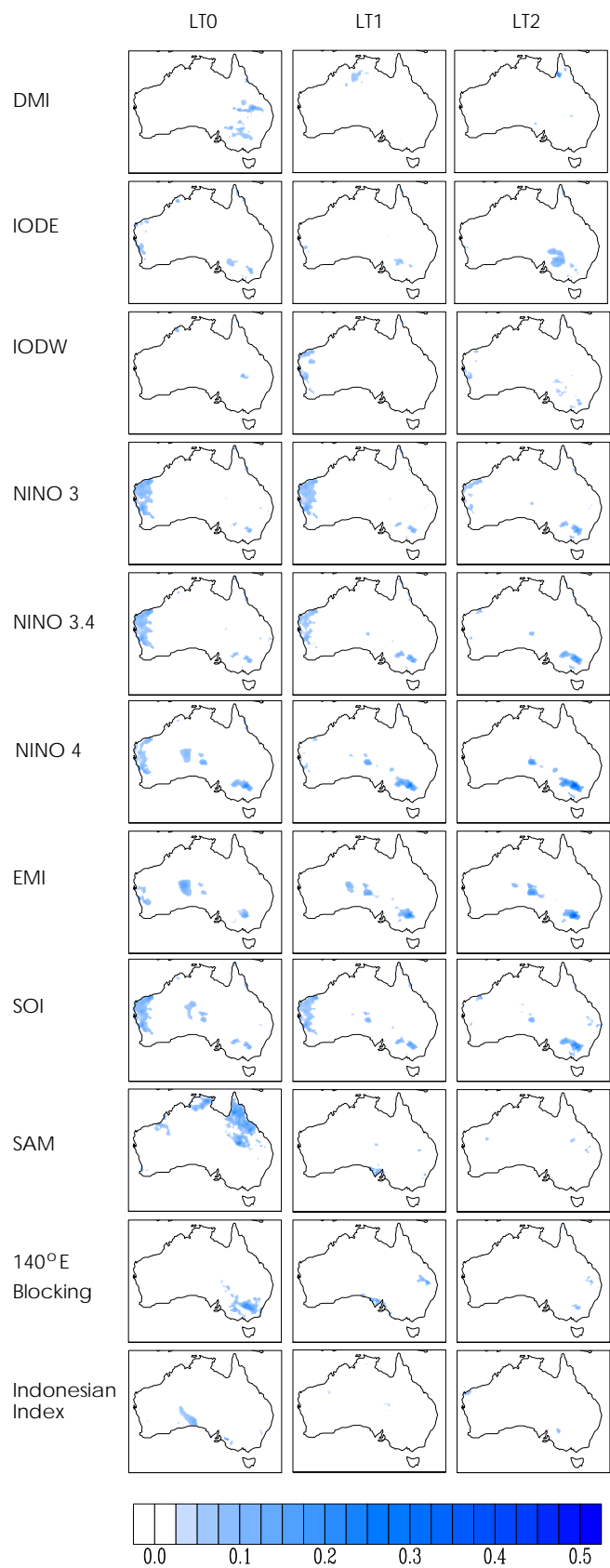


Fig. A.5 RMSE skill score for predicting Australian rainfall with POAMA predicted indices, compared to climatological rainfall, for JFM. Results for p15b, 1980-2006.

APPENDIX A

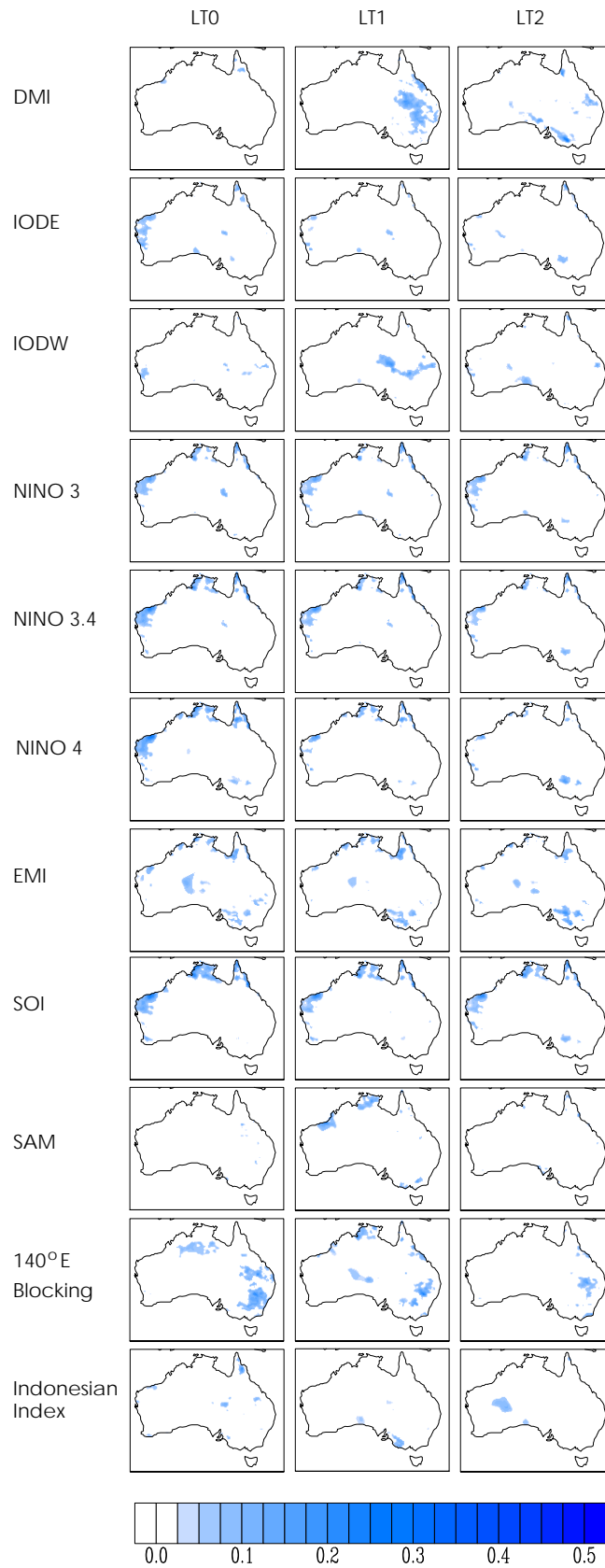


Fig. A.6 RMSE skill score for predicting Australian rainfall with POAMA predicted indices, compared to climatological rainfall, for FMA. Results for p15b, 1980-2006.

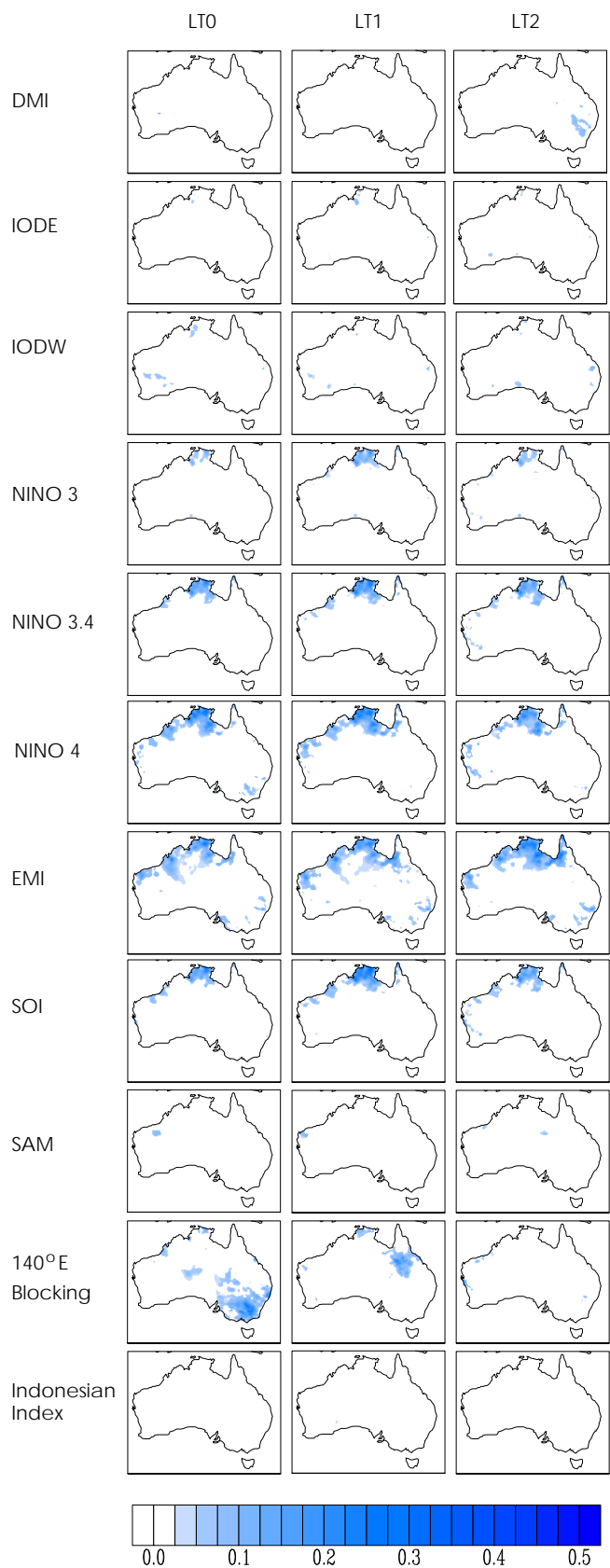


Fig. A.7 RMSE skill score for predicting Australian rainfall with POAMA predicted indices, compared to climatological rainfall, for MAM. Results for p15b, 1980-2006.

APPENDIX A

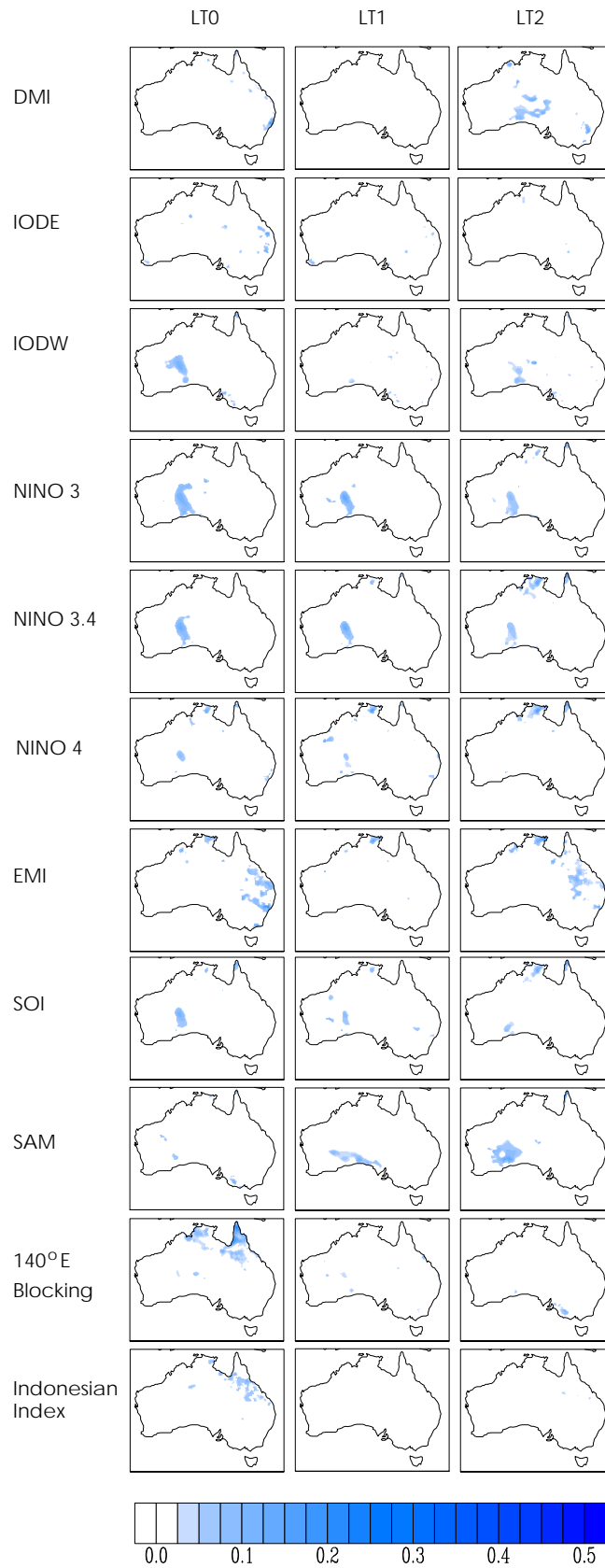


Fig. A.8 RMSE skill score for predicting Australian rainfall with POAMA predicted indices, compared to climatological rainfall, for AMJ. Results for p15b, 1980-2006.

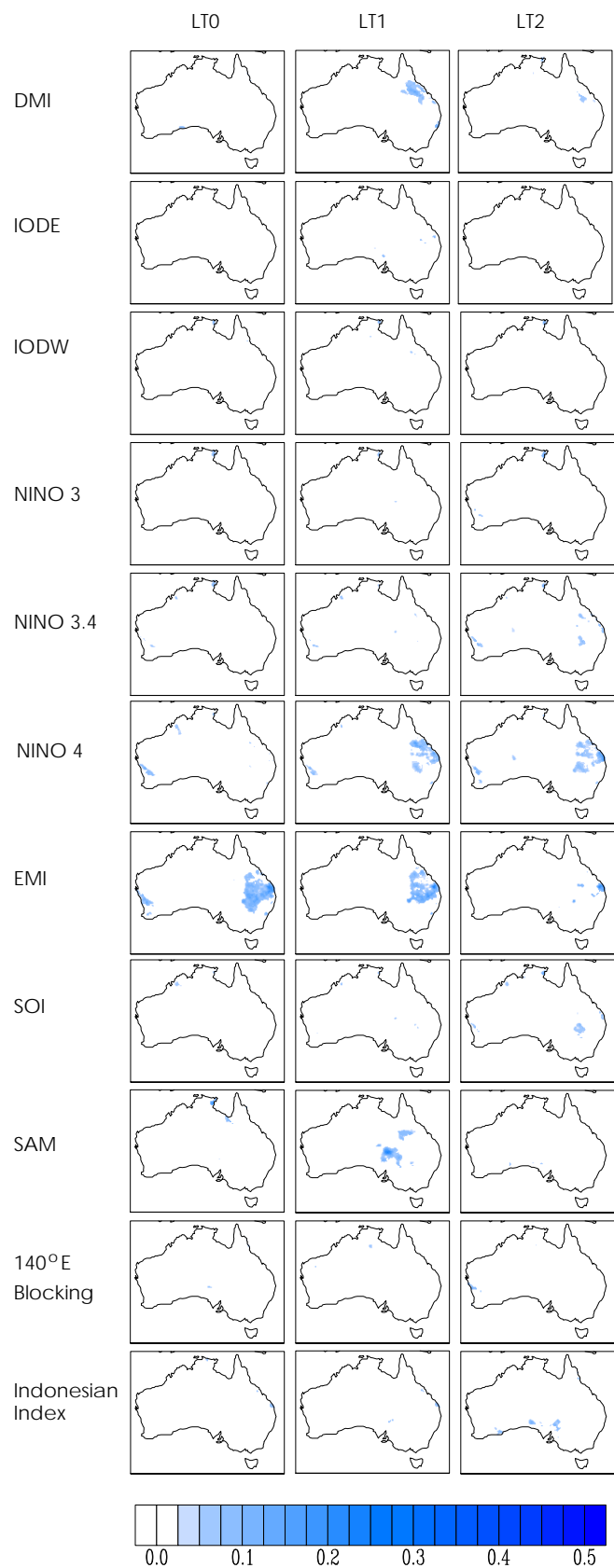


Fig. A.9 RMSE skill score for predicting Australian rainfall with POAMA predicted indices, compared to climatological rainfall, for MJJ. Results for p15b, 1980-2006.

APPENDIX A

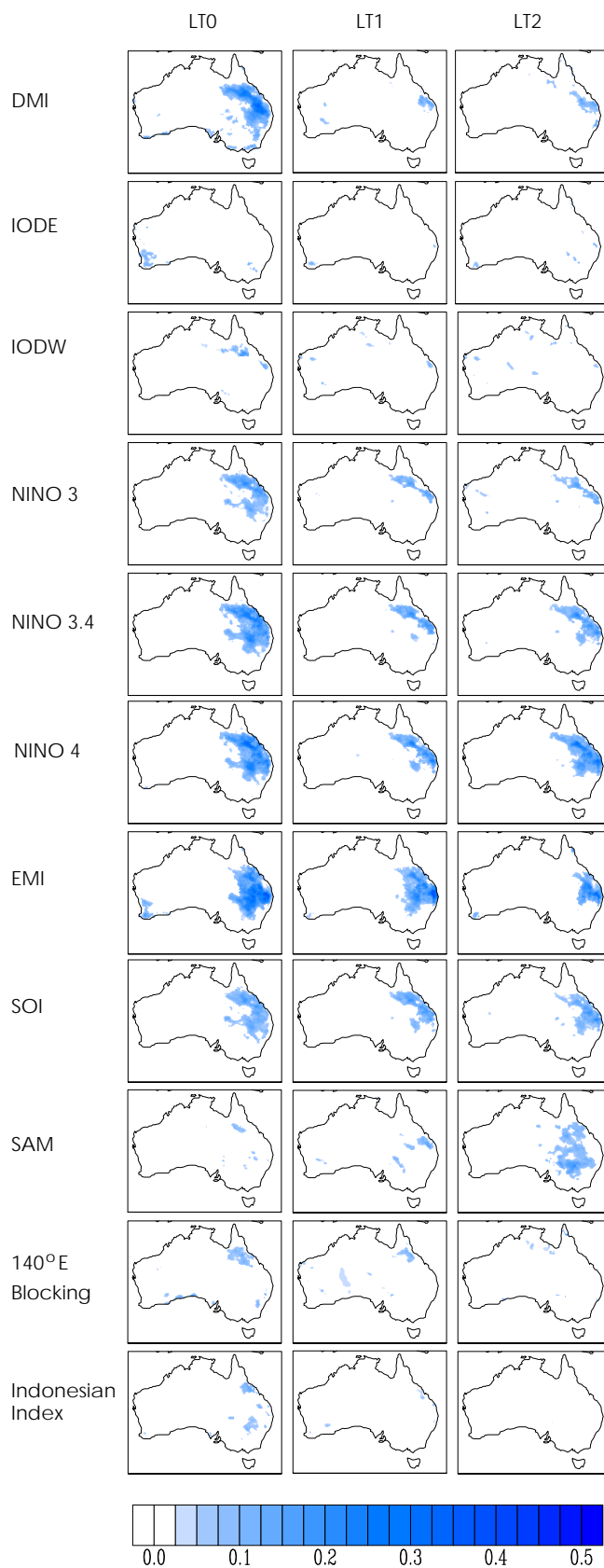


Fig. A.10 RMSE skill score for predicting Australian rainfall with POAMA predicted indices, compared to climatological rainfall, for JJA. Results for p15b, 1980-2006.

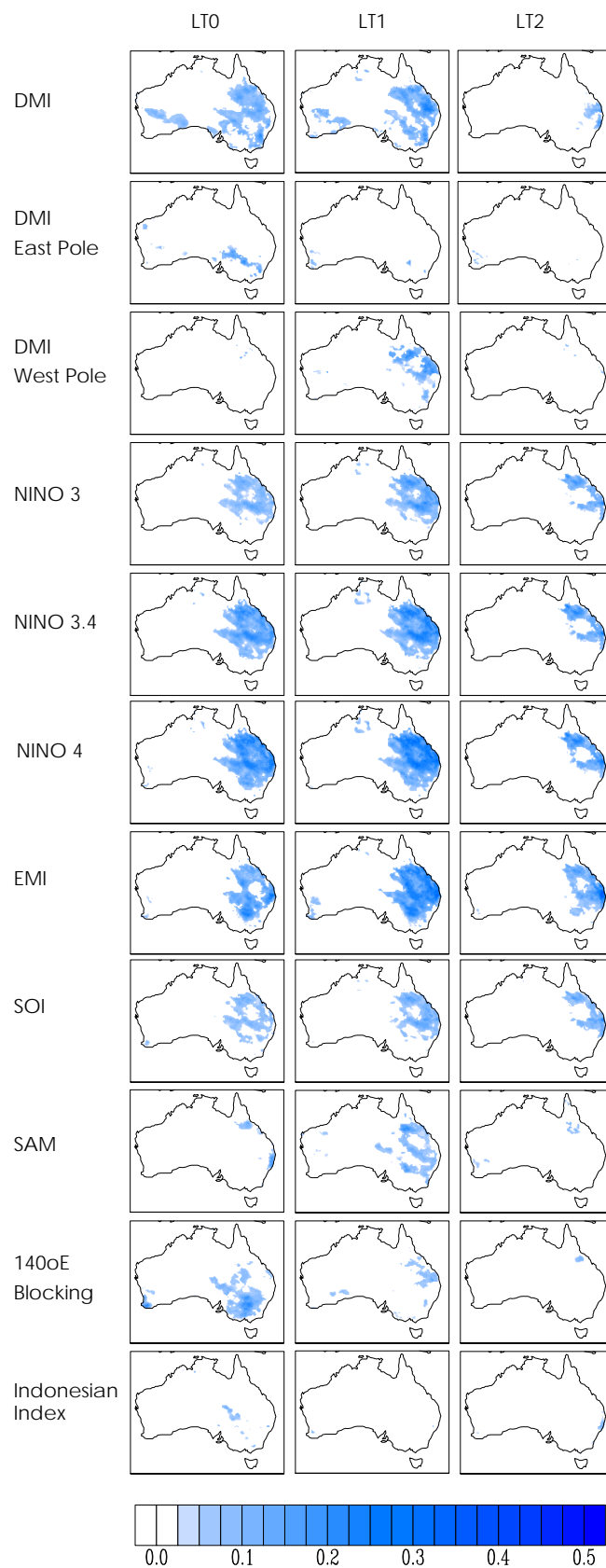


Fig. A.11 RMSE skill score for predicting Australian rainfall with POAMA predicted indices, compared to climatological rainfall, for JAS. Results for p15b, 1980-2006.

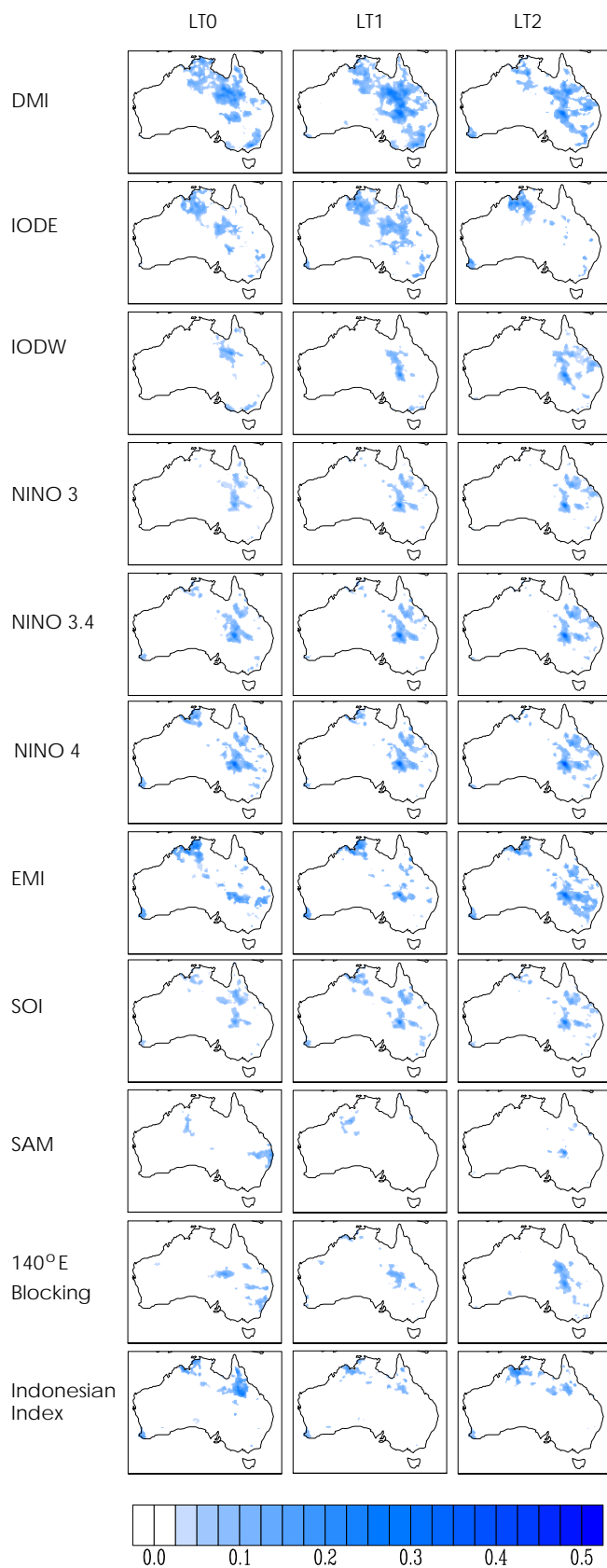


Fig. A.12 RMSE skill score for predicting Australian rainfall with POAMA predicted indices, compared to climatological rainfall, for ASO. Results for p15b, 1980-2006.

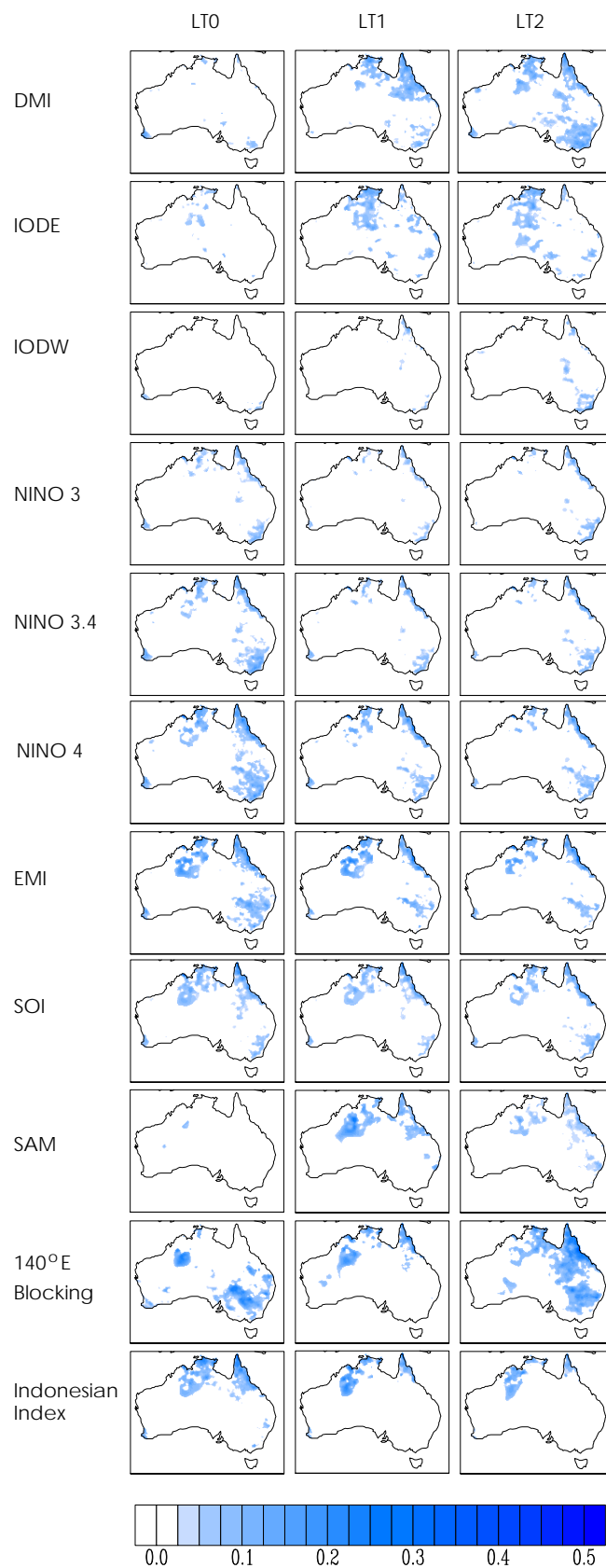


Fig. A.13 RMSE skill score for predicting Australian rainfall with POAMA predicted indices, compared to climatological rainfall, for SON. Results for p15b, 1980-2006.

APPENDIX A

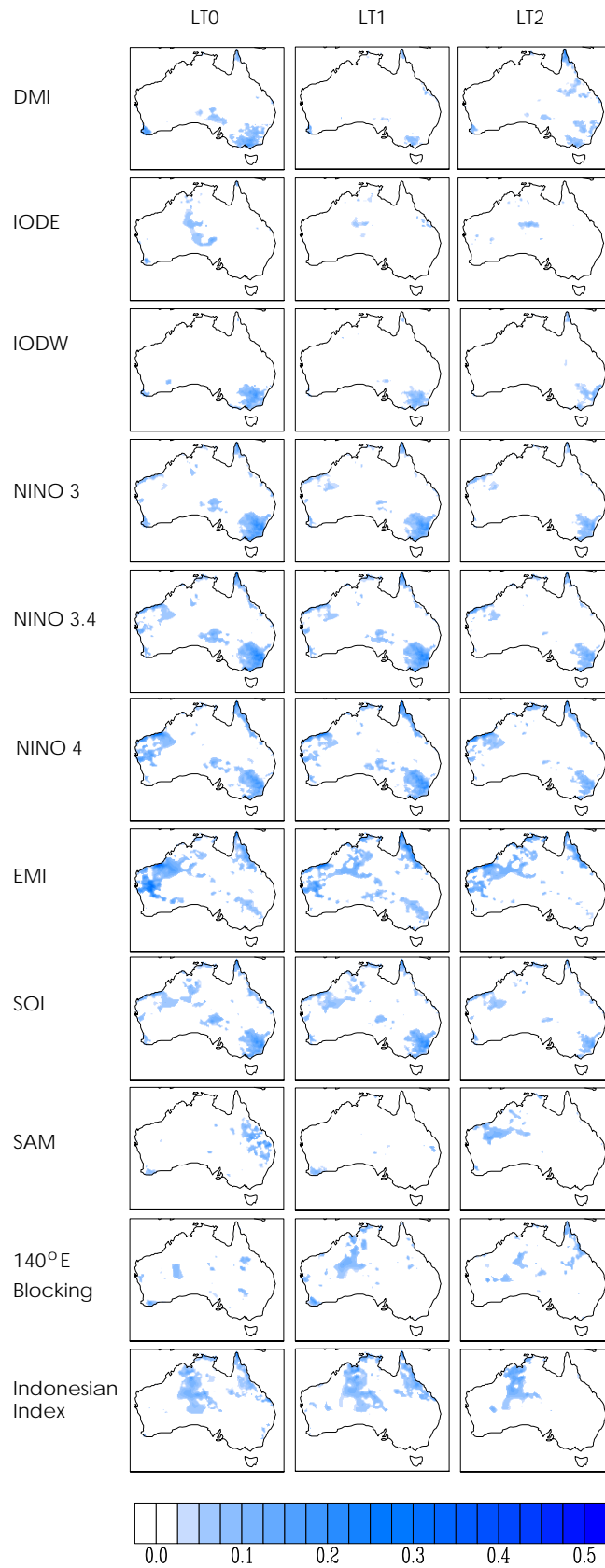


Fig. A.14 RMSE skill score for predicting Australian rainfall with POAMA predicted indices, compared to climatological rainfall, for OND. Results for p15b, 1980-2006.

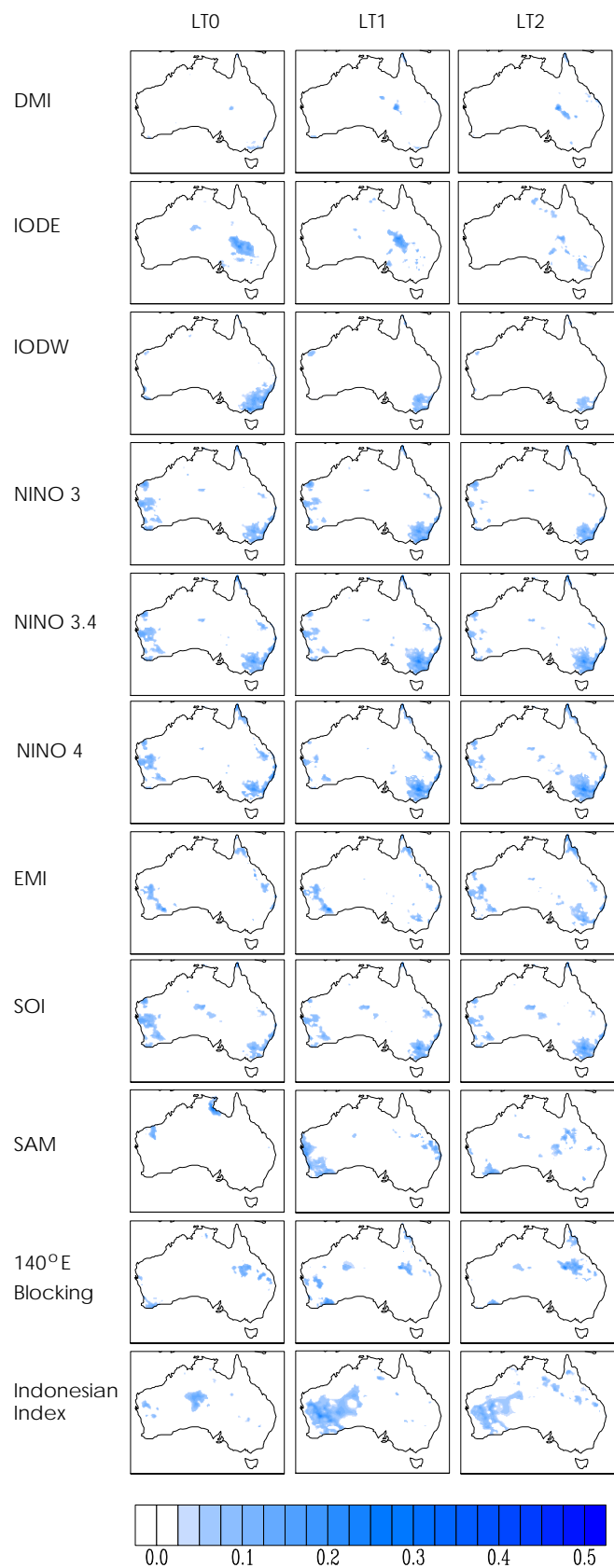


Fig. A.15 RMSE skill score for predicting Australian rainfall with POAMA predicted indices, compared to climatological rainfall, for NDJ. Results for p15b, 1980-2006.

APPENDIX A

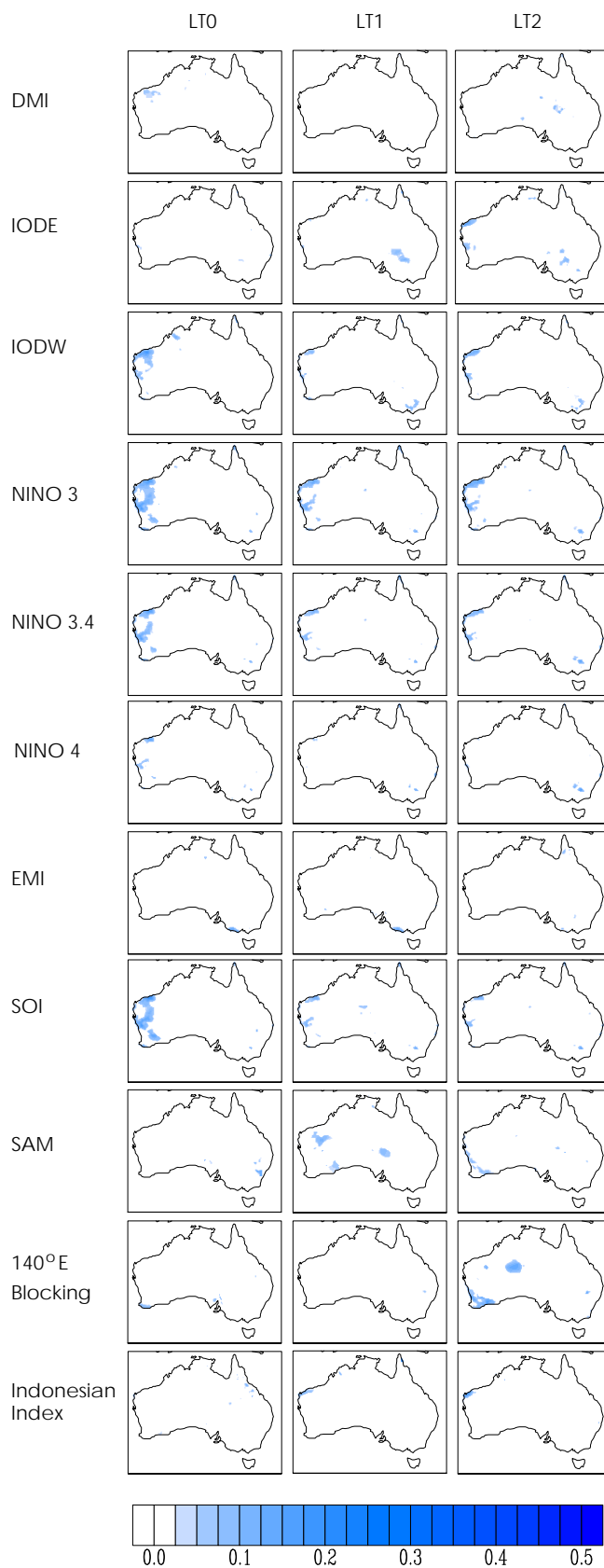


Fig. A.16 RMSE skill score for predicting Australian rainfall with POAMA predicted indices, compared to climatological rainfall, for DJF. Results for p15b, 1980-2006.

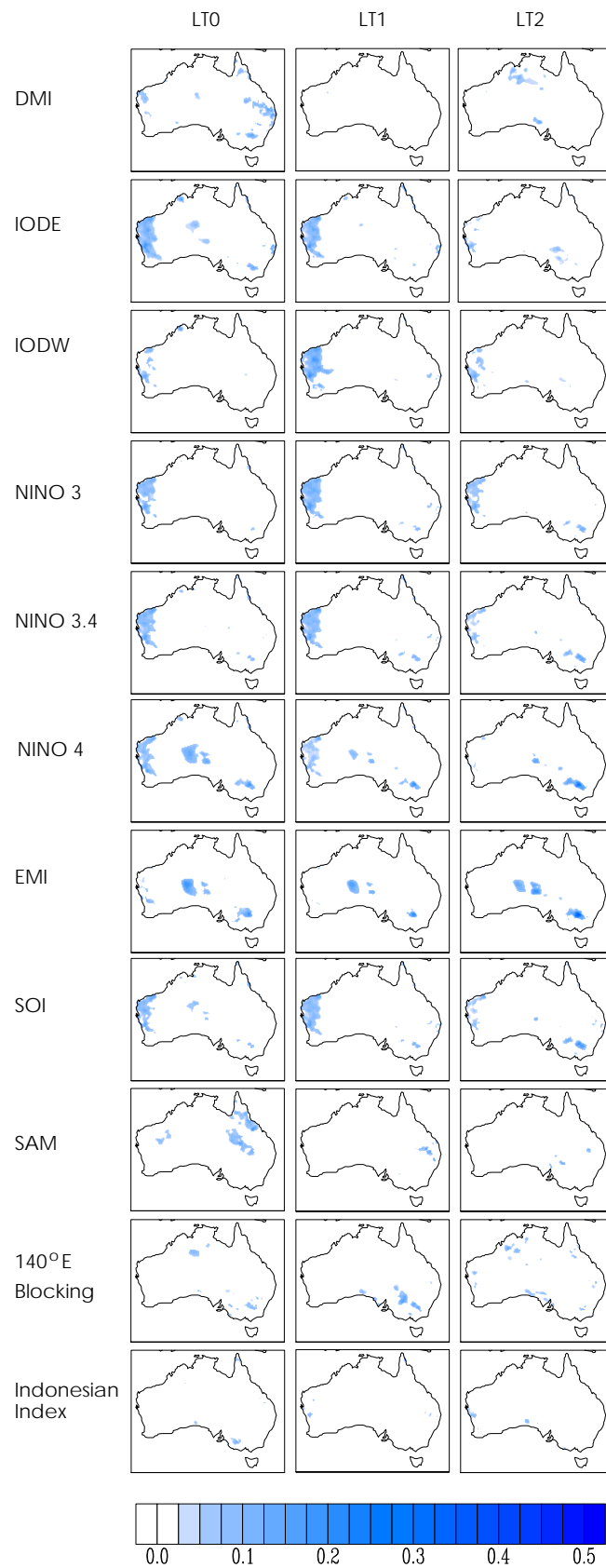


Fig. A.17 RMSE skill score for predicting Australian rainfall with POAMA predicted indices, compared to climatological rainfall, for JFM. Results for p24, 1980-2006.

APPENDIX A

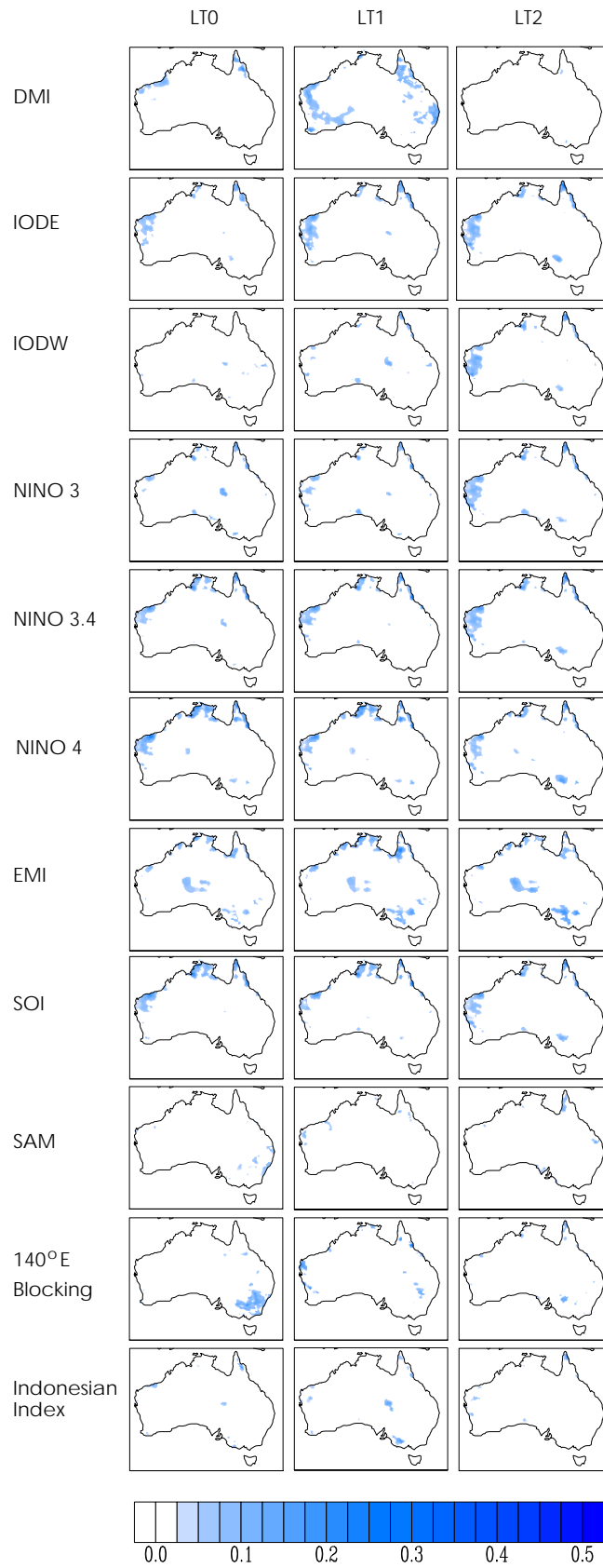


Fig. A.18 RMSE skill score for predicting Australian rainfall with POAMA predicted indices, compared to climatological rainfall, for FMA. Results for p24, 1980-2006.

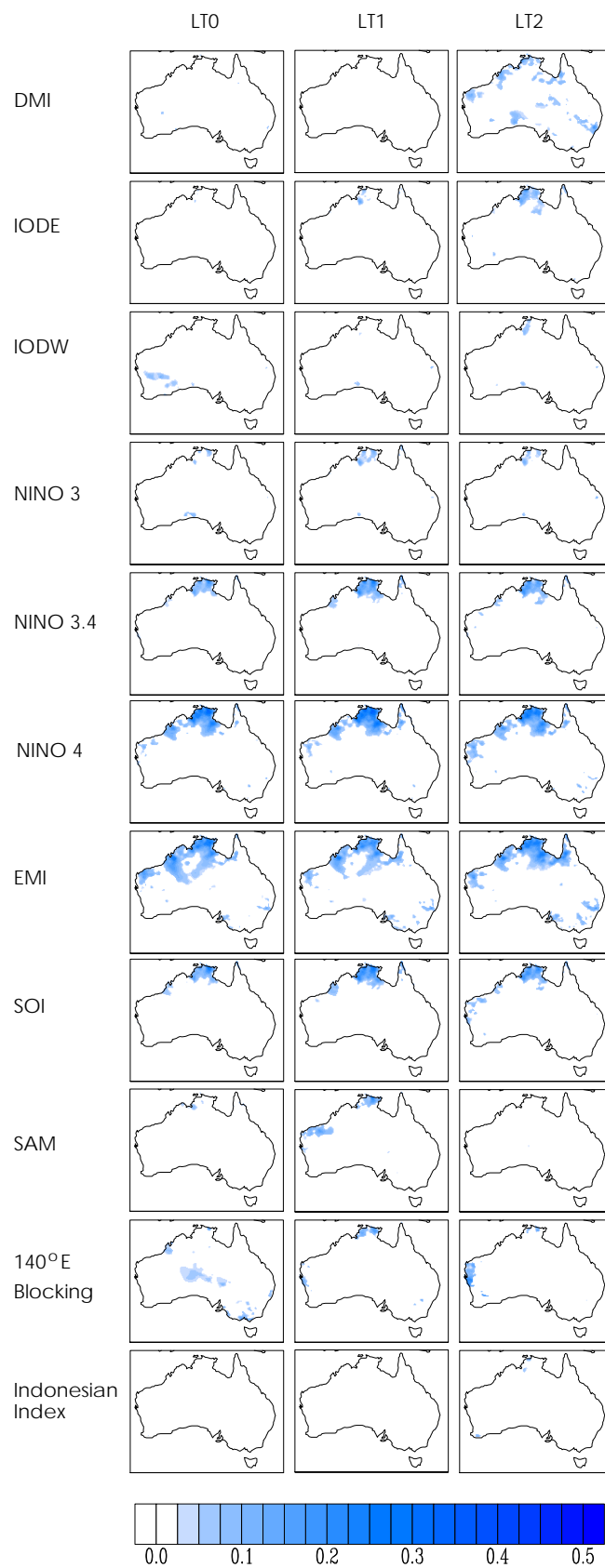


Fig. A.19 RMSE skill score for predicting Australian rainfall with POAMA predicted indices, compared to climatological rainfall, for MAM. Results for p24, 1980-2006.

APPENDIX A

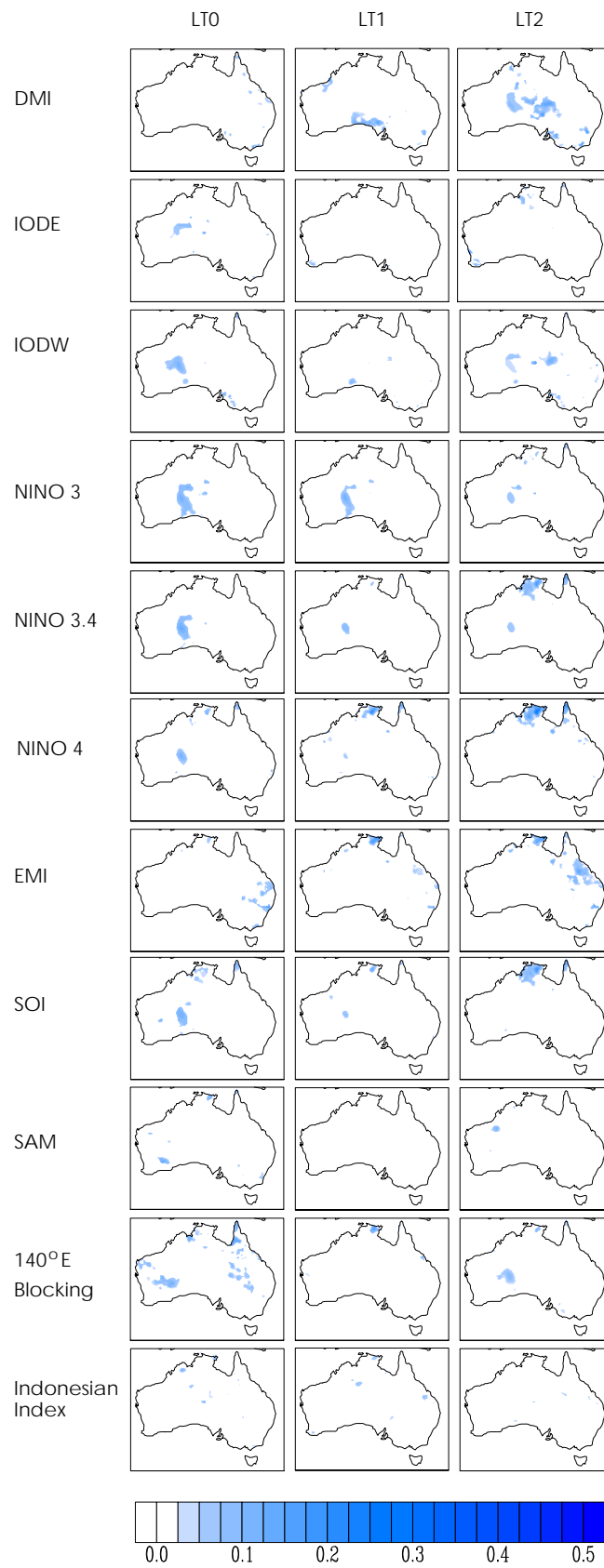


Fig. A.20 RMSE skill score for predicting Australian rainfall with POAMA predicted indices, compared to climatological rainfall, for AMJ. Results for p24, 1980-2006.

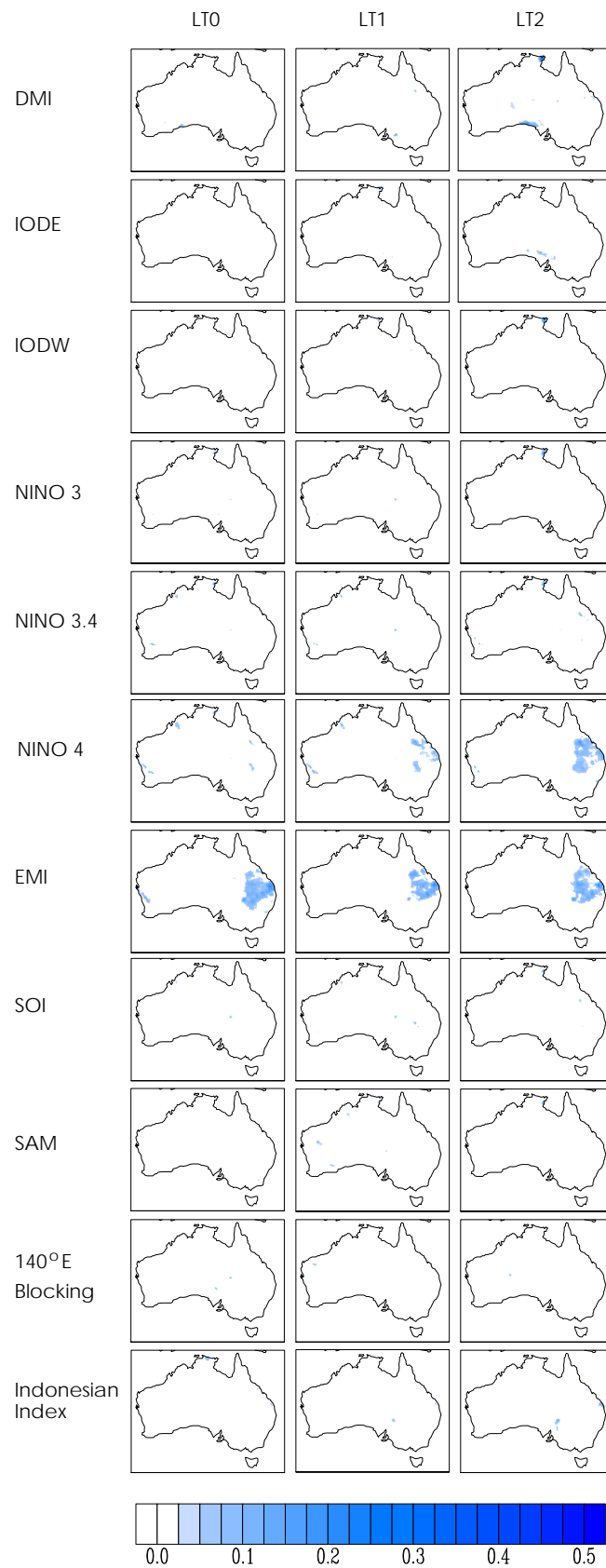


Fig. A.21 RMSE skill score for predicting Australian rainfall with POAMA predicted indices, compared to climatological rainfall, for MJJ. Results for p24, 1980-2006.

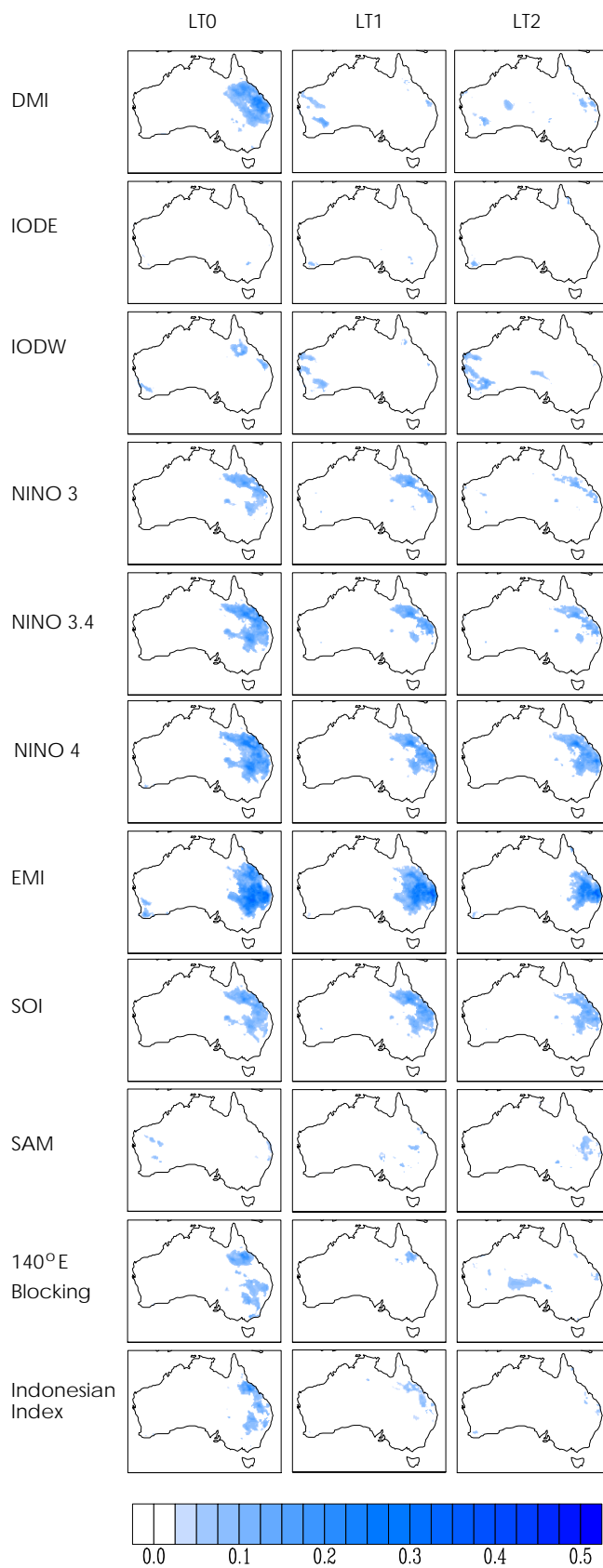


Fig. A.22 RMSE skill score for predicting Australian rainfall with POAMA predicted indices, compared to climatological rainfall, for JJA. Results for p24, 1980-2006.

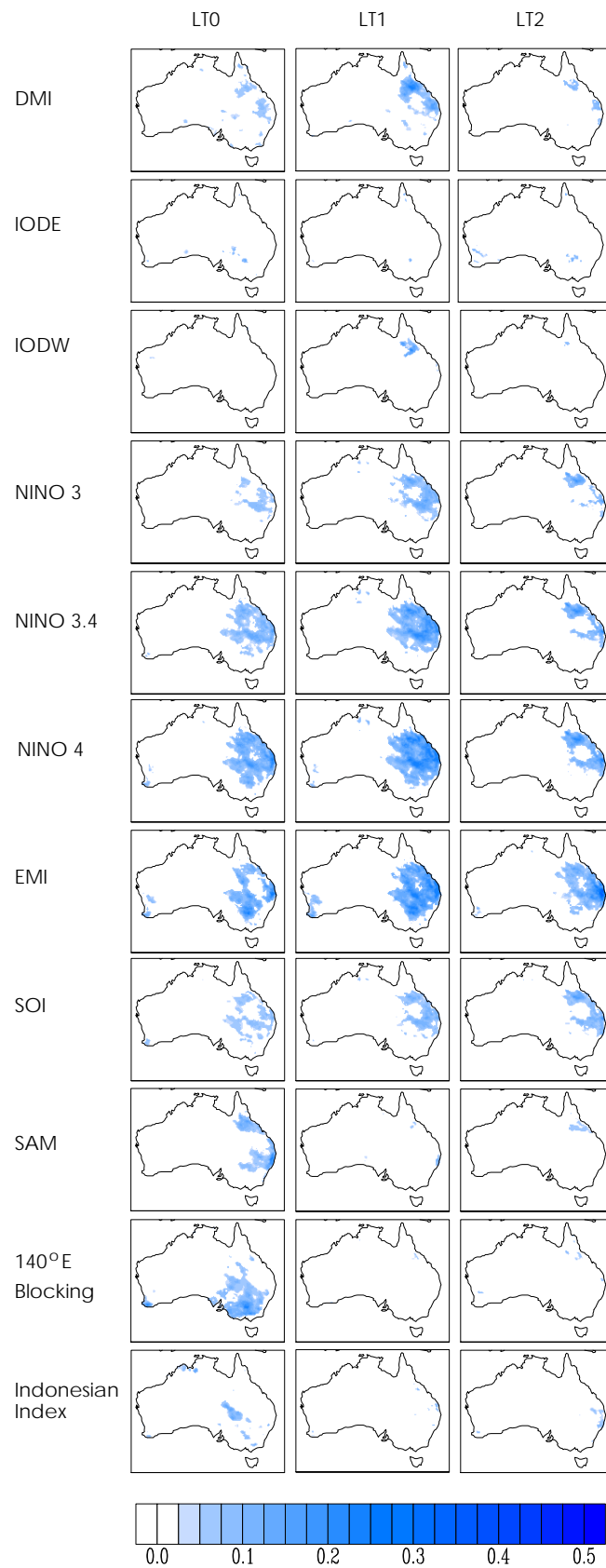


Fig. A.23 RMSE skill score for predicting Australian rainfall with POAMA predicted indices, compared to climatological rainfall, for JAS. Results for p24, 1980-2006.

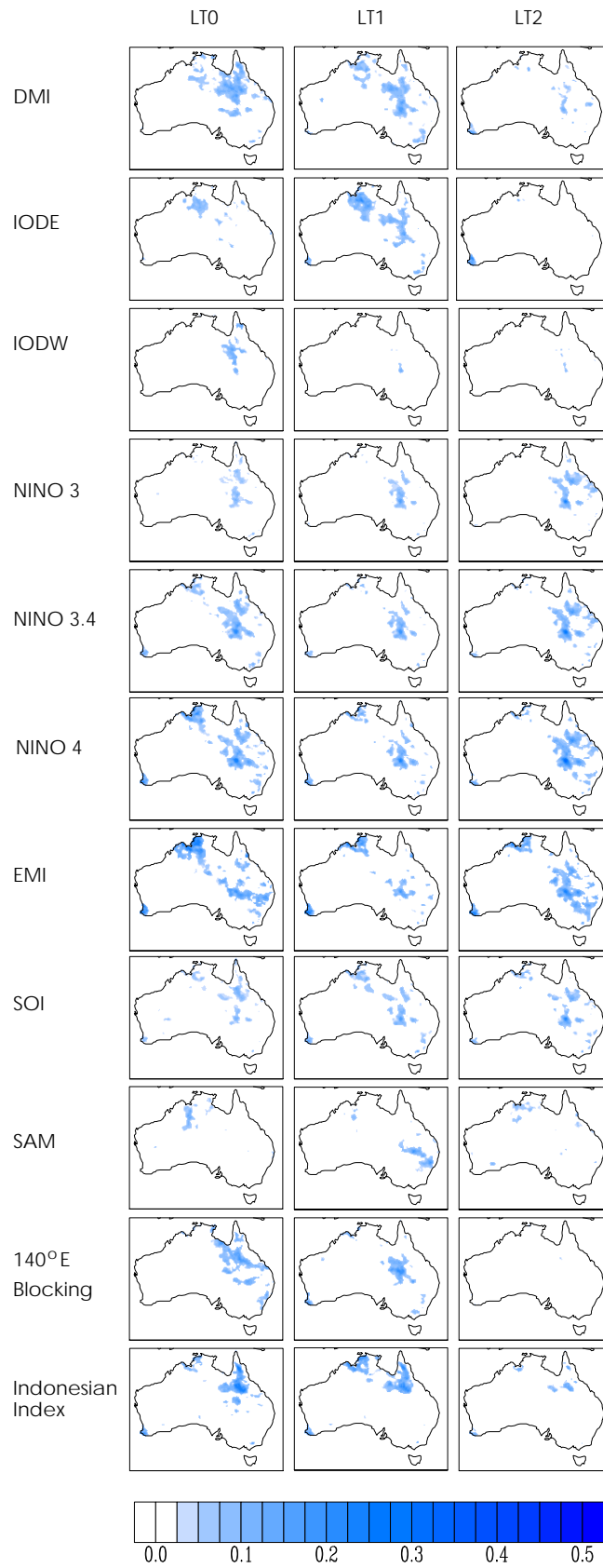


Fig. A.24 RMSE skill score for predicting Australian rainfall with POAMA predicted indices, compared to climatological rainfall, for ASO. Results for p24, 1980-2006.

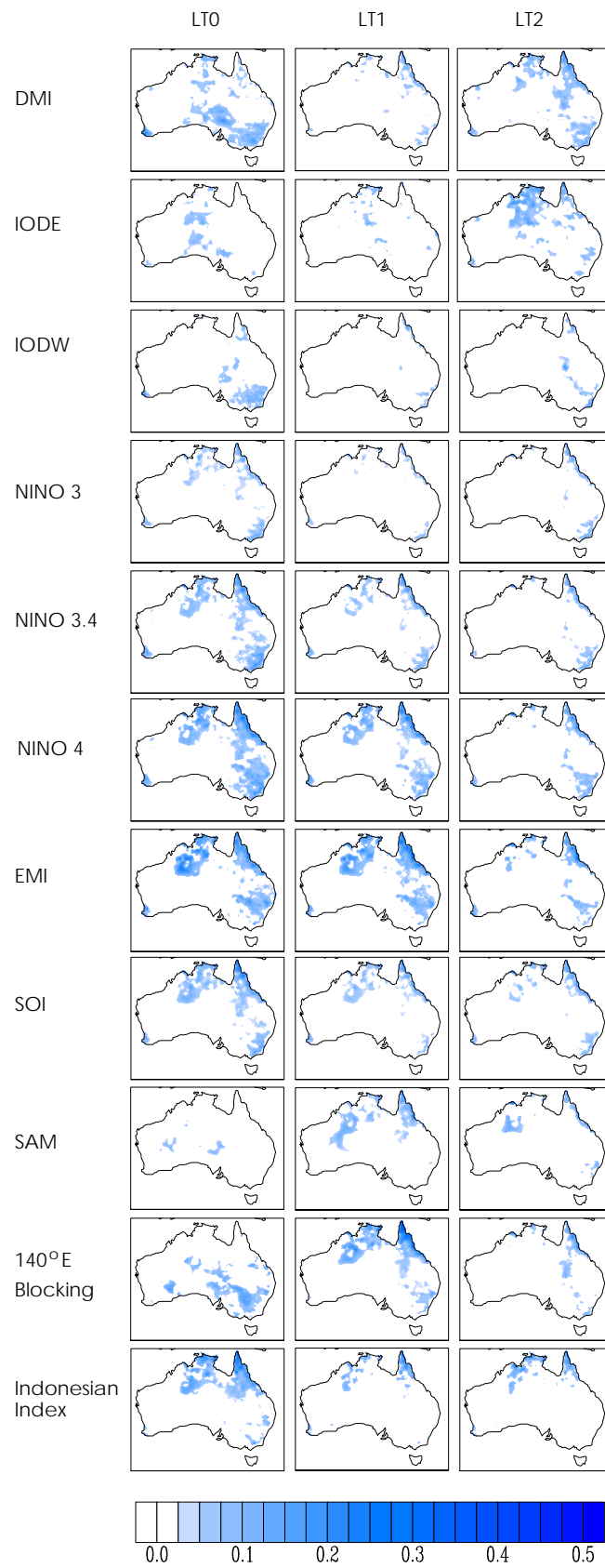


Fig. A.25 RMSE skill score for predicting Australian rainfall with POAMA predicted indices, compared to climatological rainfall, for SON. Results for p24, 1980-2006.

APPENDIX A

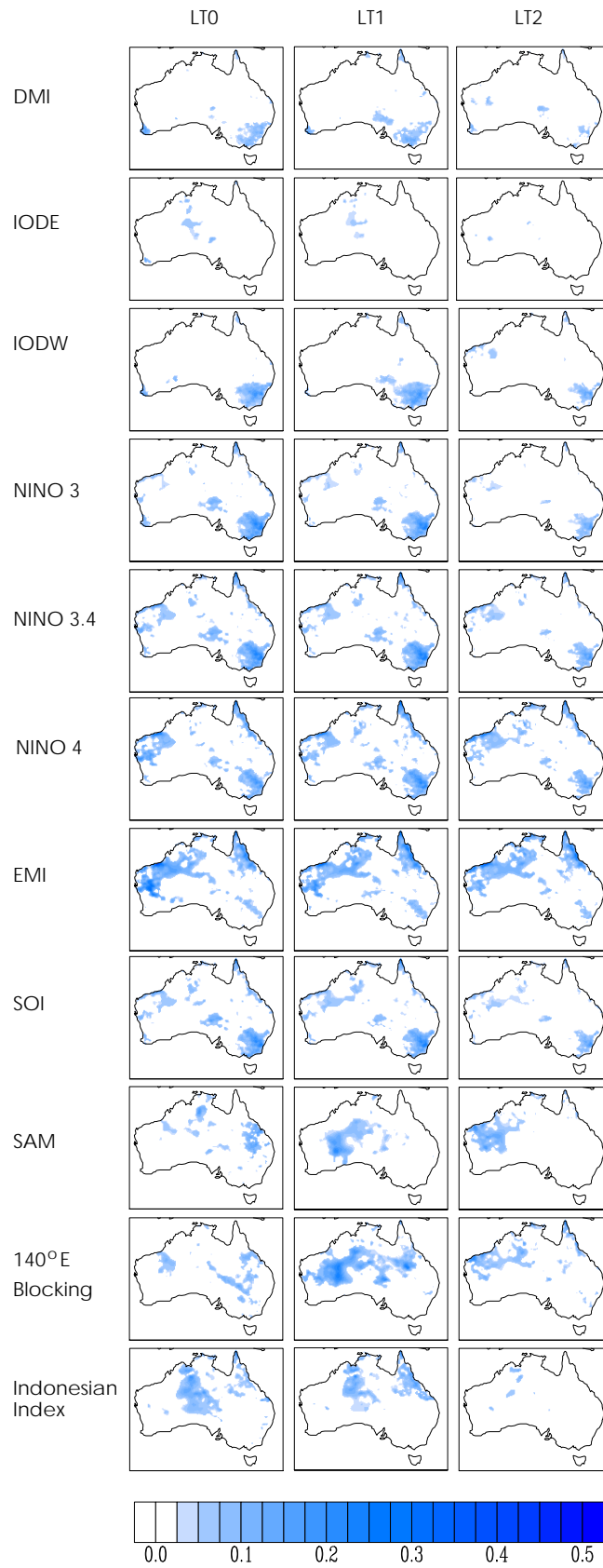


Fig. A.26 RMSE skill score for predicting Australian rainfall with POAMA predicted indices, compared to climatological rainfall, for OND. Results for p24, 1980-2006.

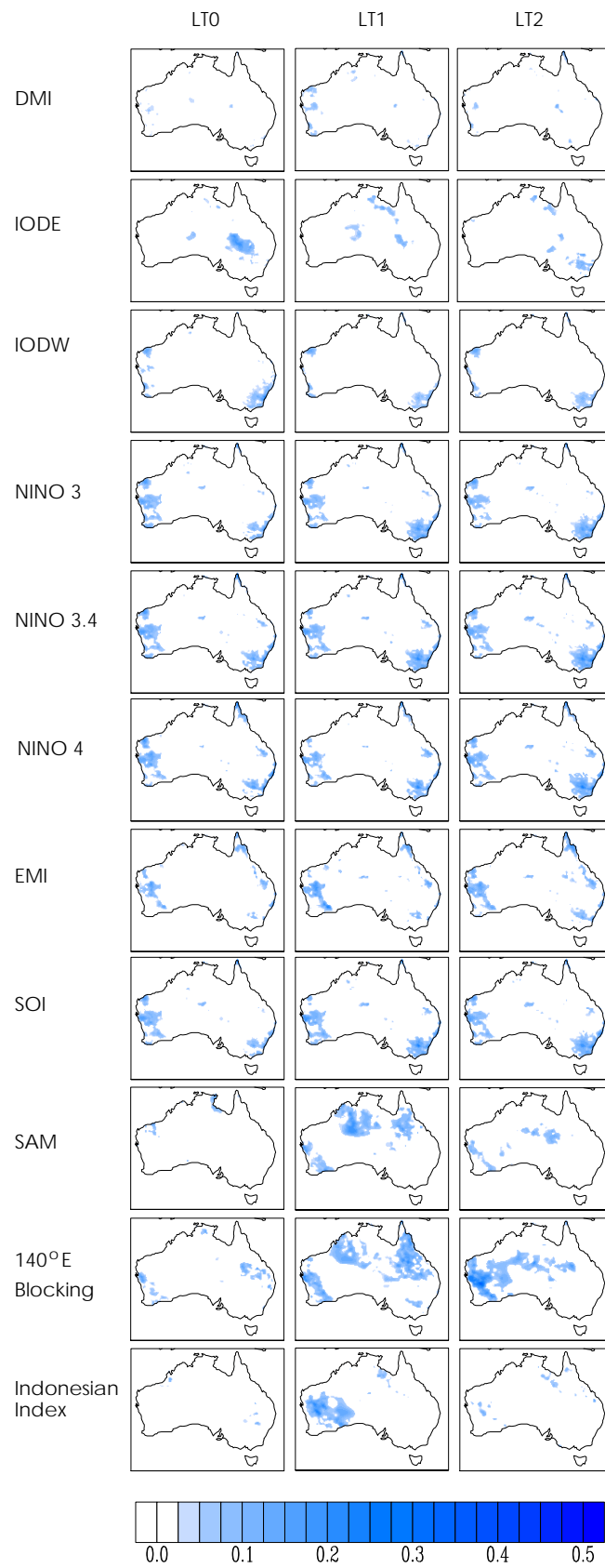


Fig. A.27 RMSE skill score for predicting Australian rainfall with POAMA predicted indices, compared to climatological rainfall, for NDJ. Results for p24, 1980-2006.

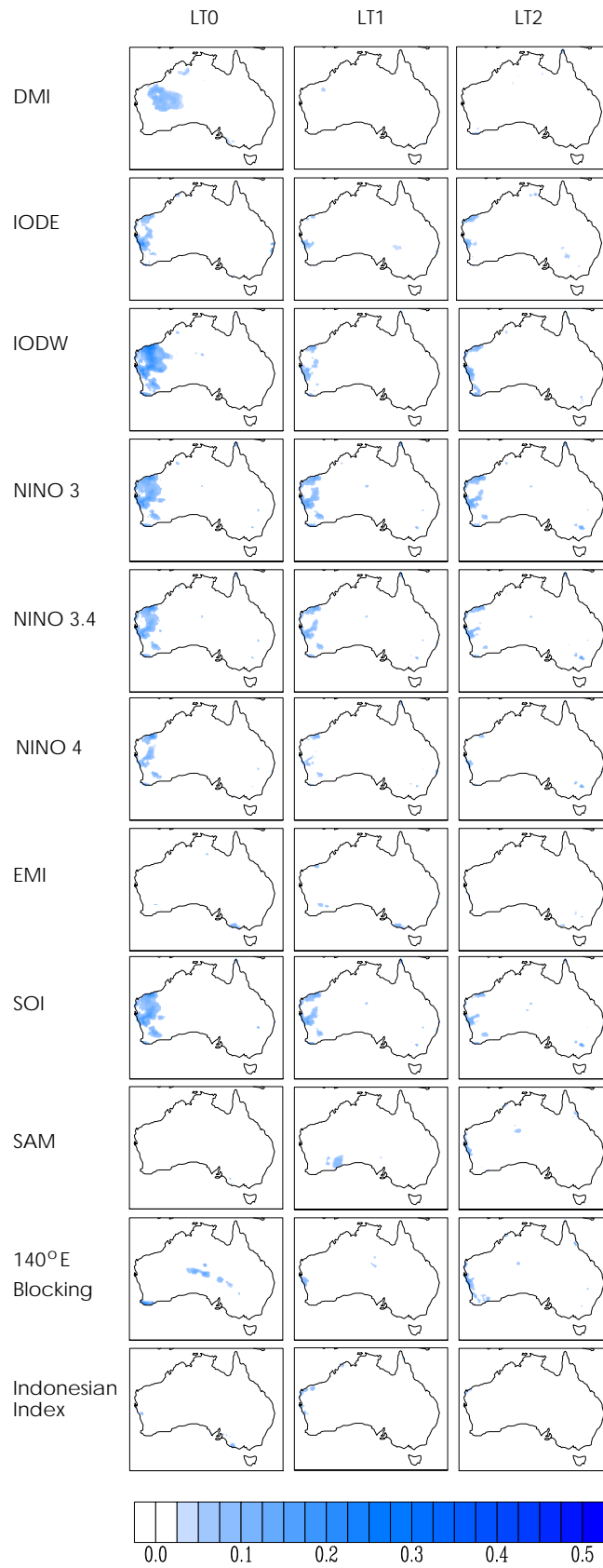


Fig. A.28 RMSE skill score for predicting Australian rainfall with POAMA predicted indices, compared to climatological rainfall, for DJF. Results for p24, 1980-2006.

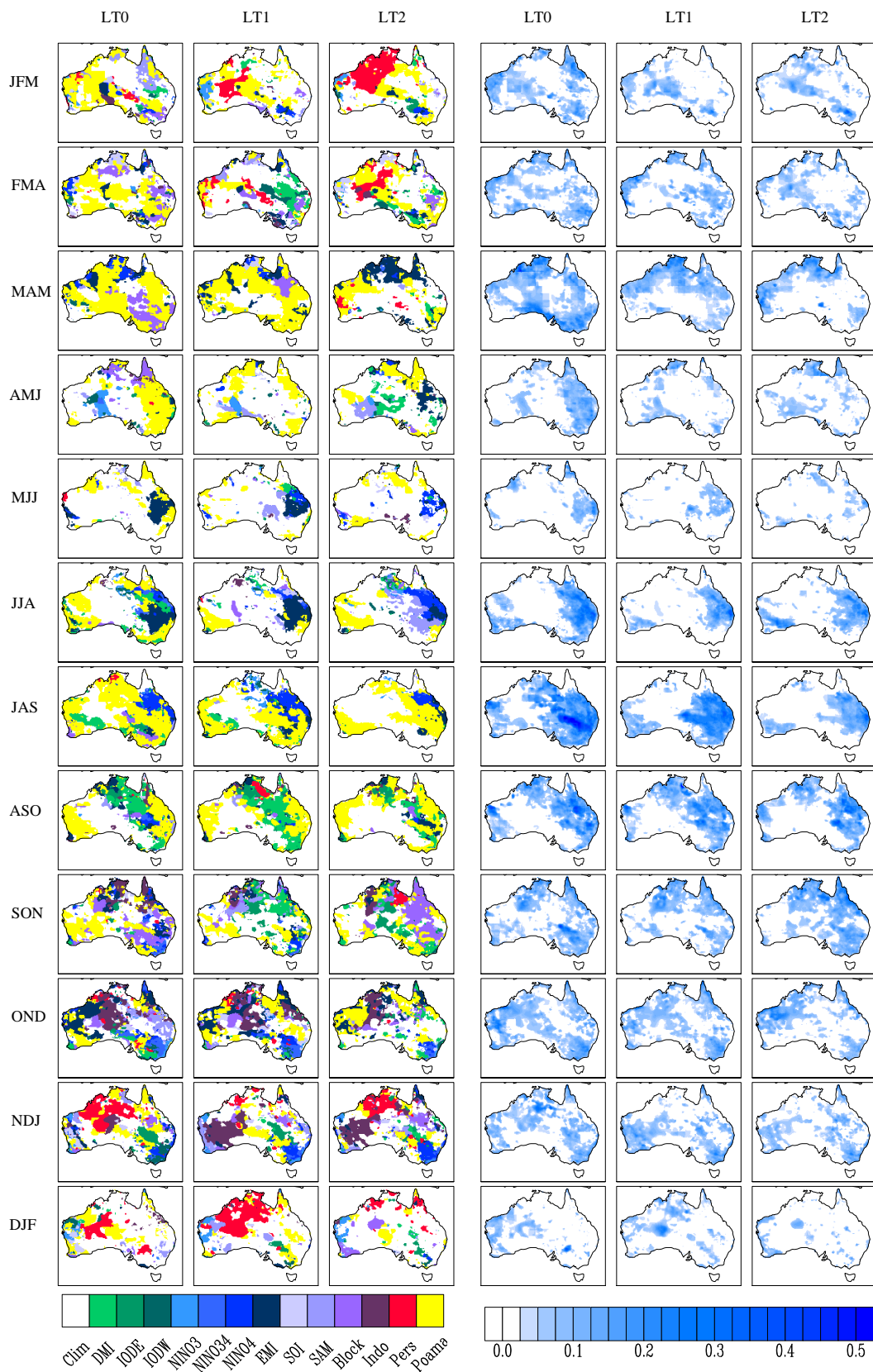


Fig. A.29 Prediction of Australian rainfall with highest RMSE skill score, compared to climatology. The corresponding highest RMSE skill score for each grid point is shown on the right. Results for POAMA version p15b, 1980-2006. Significance limit of 90 per cent.

APPENDIX A

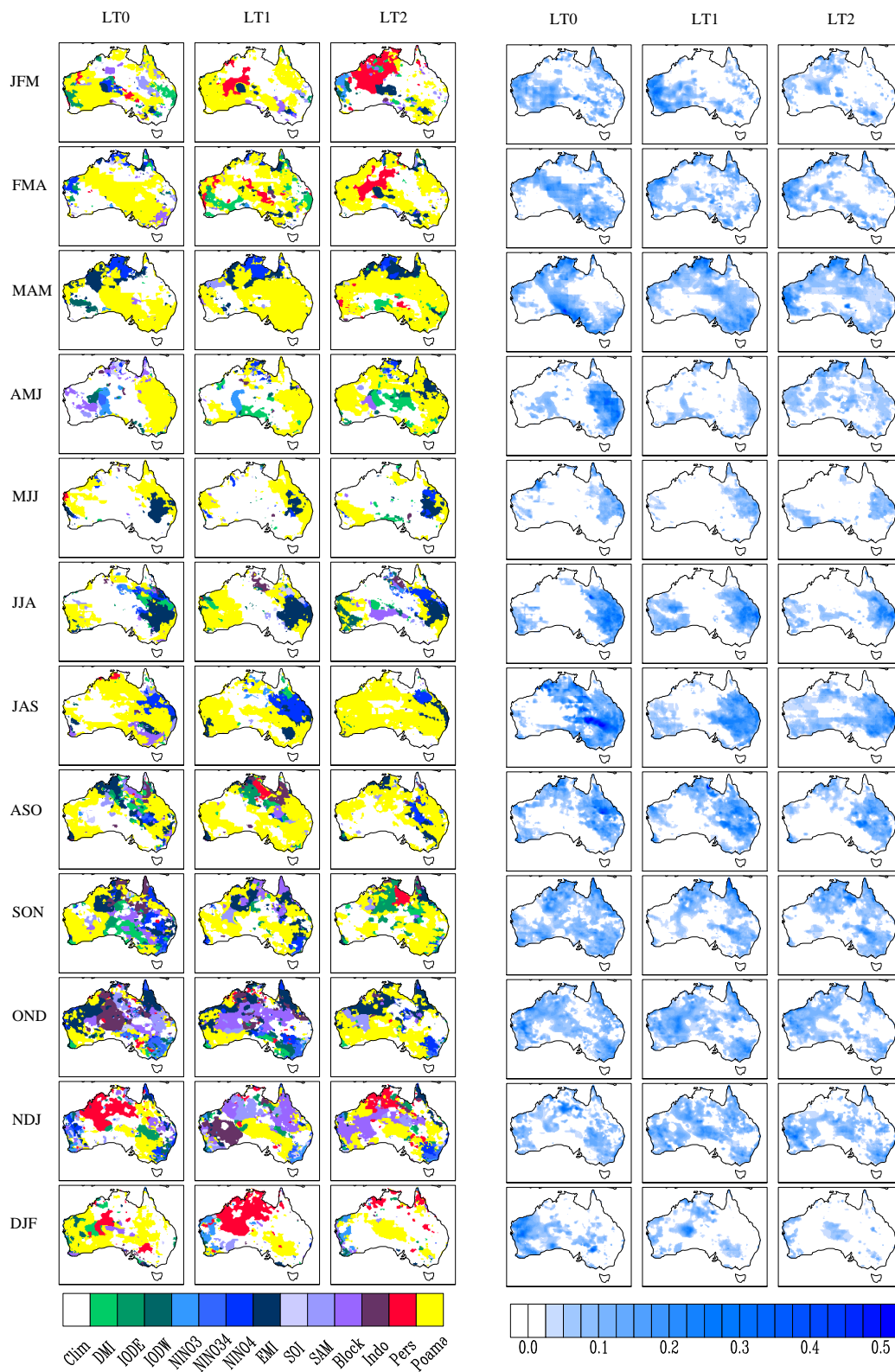


Fig. A.30 Prediction of Australian rainfall with highest RMSE skill score, compared to climatology. The corresponding highest RMSE skill score for each grid point is shown on the right. Results for POAMA version p24, 1980-2006. Significance limit of 90 per cent.

Table 1. Cross correlation of observed indices for JFM.

IODE	-0.33										
IODW	0.37	0.75									
NINO3	-0.02	0.69	0.67								
NINO3.4	-0.07	0.70	0.64	0.96							
NINO4	0.02	0.57	0.57	0.73	0.89						
EMI	-0.01	0.21	0.20	0.27	0.53	0.84					
SOI	0.20	-0.63	-0.49	-0.89	-0.95	-0.85	-0.54				
SAM	0.52	-0.05	0.31	-0.13	-0.22	-0.23	-0.34	0.35			
Block	-0.15	-0.04	-0.14	-0.36	-0.32	-0.28	-0.14	0.30	0.21		
Indo	-0.06	0.67	0.62	0.31	0.24	0.06	-0.26	-0.06	0.30	0.20	
	DMI	IODE	IOD W	NIN O3	NIN O3.4	NIN O4	EMI	SOI	SAM	Block	

Table 2. Cross correlation of observed indices for FMA.

IODE	-0.51										
IODW	0.16	0.77									
NINO3	-0.22	0.69	0.62								
NINO3.4	-0.25	0.68	0.60	0.94							
NINO4	-0.12	0.53	0.52	0.67	0.87						
EMI	-0.02	0.10	0.10	0.12	0.44	0.80					
SOI	0.32	-0.56	-0.40	-0.83	-0.92	-0.85	-0.51				
SAM	0.37	0.07	0.36	0.02	-0.13	-0.24	-0.37	0.32			
Block	-0.44	0.23	-0.06	-0.16	-0.14	-0.19	-0.14	0.20	0.18		
Indo	-0.25	0.71	0.63	0.31	0.23	0.04	-0.32	0.00	0.31	0.42	
	DMI	IODE	IOD W	NIN O3	NIN O3.4	NIN O4	EMI	SOI	SAM	Block	

Table 3. Cross correlation of observed indices for MAM.

IODE	-0.52										
IODW	0.25	0.69									
NINO3	-0.11	0.62	0.61								
NINO3.4	-0.11	0.60	0.58	0.93							
NINO4	0.00	0.45	0.51	0.66	0.87						
EMI	0.13	-0.09	0.01	-0.05	0.29	0.69					
SOI	0.18	-0.44	-0.35	-0.82	-0.90	-0.81	-0.35				
SAM	0.25	-0.02	0.19	-0.09	-0.24	-0.31	-0.35	0.44			
Block	-0.42	0.25	-0.07	-0.17	-0.17	-0.18	-0.16	0.15	0.07		
Indo	-0.52	0.70	0.35	0.09	0.03	-0.07	-0.37	0.14	-0.02	0.36	
	DMI	IODE	IOD W	NIN O3	NIN O3.4	NIN O4	EMI	SOI	SAM	Block	

Table 4. Cross correlation of observed indices for AMJ.

IODE	-0.43										
IODW	0.49	0.58									
NINO3	0.22	0.40	0.59								
NINO3.4	0.21	0.36	0.54	0.93							
NINO4	0.24	0.30	0.51	0.70	0.90						
EMI	0.10	-0.20	-0.10	-0.10	0.25	0.59					
SOI	-0.13	-0.29	-0.40	-0.86	-0.90	-0.76	-0.16				
SAM	0.13	0.01	0.13	-0.08	-0.23	-0.29	-0.33	0.31			
Block	-0.46	0.41	-0.02	-0.25	-0.27	-0.21	-0.14	0.23	0.13		
Indo	-0.60	0.65	0.08	-0.16	-0.25	-0.25	-0.39	0.31	0.01	0.51	
	DMI	IODE	IOD W	NIN O3	NIN O3.4	NIN O4	EMI	SOI	SAM	Block	

Table 5. Cross correlation of observed indices for MJJ.

IODE	-0.47										
IODW	0.56	0.47									
NINO3	0.45	0.13	0.57								
NINO3.4	0.39	0.06	0.44	0.92							
NINO4	0.34	0.10	0.43	0.72	0.91						
EMI	-0.05	-0.22	-0.26	-0.11	0.28	0.55					
SOI	-0.40	0.03	-0.38	-0.85	-0.87	-0.71	-0.10				
SAM	-0.02	0.07	0.05	-0.03	-0.17	-0.26	-0.38	0.21			
Block	-0.12	0.24	0.11	-0.09	-0.15	-0.16	-0.20	0.20	0.23		
Indo	-0.61	0.69	0.04	-0.33	-0.42	-0.34	-0.33	0.52	0.12	0.32	
	DMI	IODE	IODW	NINO3	NINO3.4	NINO4	EMI	SOI	SAM	Block	

Table 6. Cross correlation of observed indices for JJA.

IODE	-0.63										
IODW	0.56	0.28									
NINO3	0.50	-0.16	0.45								
NINO3.4	0.43	-0.26	0.26	0.90							
NINO4	0.36	-0.16	0.27	0.69	0.90						
EMI	-0.04	-0.28	-0.35	-0.06	0.37	0.62					
SOI	-0.47	0.26	-0.31	-0.89	-0.87	-0.69	-0.11				
SAM	0.19	0.11	0.35	0.12	0.00	-0.03	-0.27	-0.15			
Block	-0.33	0.20	-0.20	-0.28	-0.44	-0.58	-0.48	0.44	0.10		
Indo	-0.69	0.77	-0.04	-0.45	-0.55	-0.47	-0.37	0.63	0.01	0.54	
	DMI	IODE	IODW	NINO3	NINO3.4	NINO4	EMI	SOI	SAM	Block	

Table 7. Cross correlation of observed indices for JAS.

IODE	-0.78										
IODW	0.57	0.07									
NINO3	0.59	-0.38	0.43								
NINO3.4	0.55	-0.46	0.27	0.92							
NINO4	0.44	-0.37	0.21	0.68	0.89						
EMI	0.08	-0.31	-0.28	0.01	0.40	0.69					
SOI	-0.61	0.46	-0.37	-0.93	-0.91	-0.73	-0.17				
SAM	0.24	-0.01	0.37	0.07	0.05	0.12	-0.02	-0.14			
Block	-0.13	0.06	-0.13	-0.12	-0.19	-0.30	-0.24	0.15	0.41		
Indo	-0.76	0.81	-0.15	-0.60	-0.68	-0.59	-0.39	0.74	-0.08	0.20	
	DMI	IODE	IOD W	NIN O3	NIN O3.4	NIN O4	EMI	SOI	SAM	Block	

Table 8. Cross correlation of observed indices for ASO.

IODE	-0.84										
IODW	0.67	-0.16									
NINO3	0.70	-0.57	0.50								
NINO3.4	0.70	-0.62	0.43	0.95							
NINO4	0.59	-0.52	0.35	0.75	0.91						
EMI	0.21	-0.34	-0.09	0.17	0.46	0.75					
SOI	-0.71	0.63	-0.43	-0.94	-0.92	-0.75	-0.24				
SAM	0.15	-0.05	0.21	0.04	0.04	0.14	0.06	-0.03			
Block	-0.07	0.01	-0.12	-0.06	-0.05	-0.05	-0.01	0.00	0.46		
Indo	-0.79	0.86	-0.28	-0.71	-0.75	-0.68	-0.43	0.79	-0.06	0.17	
	DMI	IODE	IOD W	NIN O3	NIN O3.4	NIN O4	EMI	SOI	SAM	Block	

Table 9. Cross correlation of observed indices for SON.

IODE	-0.85										
IODW	0.76	-0.31									
NINO3	0.78	-0.66	0.59								
NINO3.4	0.75	-0.65	0.56	0.96							
NINO4	0.62	-0.52	0.48	0.80	0.92						
EMI	0.19	-0.24	0.05	0.27	0.51	0.77					
SOI	-0.71	0.66	-0.47	-0.94	-0.90	-0.75	-0.29				
SAM	-0.09	0.14	0.01	-0.24	-0.23	-0.13	-0.05	0.25			
Block	-0.17	0.14	-0.14	-0.33	-0.30	-0.24	-0.09	0.18	0.60		
Indo	-0.78	0.86	-0.36	-0.78	-0.78	-0.66	-0.35	0.78	0.22	0.34	
	DMI	IODE	IODW	NINO3	NINO3.4	NINO4	EMI	SOI	SAM	Block	

Table 10. Cross correlation of observed indices for OND.

IODE	-0.80										
IODW	0.83	-0.32									
NINO3	0.77	-0.58	0.67								
NINO3.4	0.71	-0.52	0.63	0.97							
NINO4	0.56	-0.35	0.56	0.81	0.93						
EMI	0.07	-0.01	0.11	0.28	0.51	0.76					
SOI	-0.61	0.52	-0.48	-0.89	-0.87	-0.75	-0.30				
SAM	-0.17	0.21	-0.07	-0.39	-0.41	-0.32	-0.22	0.41			
Block	-0.40	0.34	-0.32	-0.46	-0.40	-0.25	0.02	0.28	0.57		
Indo	-0.63	0.75	-0.29	-0.67	-0.61	-0.46	-0.14	0.67	0.34	0.48	
	DMI	IODE	IODW	NINO3	NINO3.4	NINO4	EMI	SOI	SAM	Block	

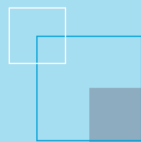
APPENDIX A

Table 11. Cross correlation of observed indices for NDJ.

IODE	-0.42										
IODW	0.81	0.19									
NINO3	0.65	-0.03	0.69								
NINO3.4	0.59	0.04	0.67	0.97							
NINO4	0.49	0.14	0.62	0.80	0.92						
EMI	0.04	0.22	0.18	0.26	0.49	0.77					
SOI	-0.48	-0.02	-0.53	-0.90	-0.91	-0.78	-0.37				
SAM	0.15	-0.07	0.12	-0.35	-0.39	-0.32	-0.25	0.48			
Block	-0.23	-0.04	-0.27	-0.56	-0.54	-0.44	-0.18	0.41	0.55		
Indo	-0.29	0.54	0.04	-0.41	-0.35	-0.21	-0.01	0.47	0.34	0.29	
	DMI	IODE	IODW	NIN O3	NIN O3.4	NIN O4	EMI	SOI	SAM	Block	

Table 12. Cross correlation of observed indices for DJF.

IODE	-0.13										
IODW	0.67	0.65									
NINO3	0.39	0.56	0.71								
NINO3.4	0.32	0.60	0.70	0.96							
NINO4	0.30	0.56	0.65	0.77	0.90						
EMI	0.03	0.31	0.25	0.28	0.51	0.81					
SOI	-0.20	-0.57	-0.58	-0.91	-0.94	-0.83	-0.48				
SAM	0.50	-0.26	0.19	-0.26	-0.30	-0.22	-0.19	0.40			
Block	-0.17	0.03	-0.10	-0.32	-0.27	-0.17	0.01	0.21	0.32		
Indo	0.04	0.61	0.49	0.19	0.18	0.11	-0.10	-0.04	0.12	0.05	
	DMI	IODE	IOD W	NIN O3	NIN O3.4	NIN O4	EMI	SOI	SAM	Block	



The Centre for Australian Weather and Climate Research is a partnership between CSIRO and the Bureau of Meteorology.